TECHNISCHE HOGESCHOOL DELFT
AFDELING DER MARITIEME TECHNIEK
LABORATORIUM VOOR SCHEEPSHYDROMECHANICA

THE HIGH-SPEED DISPLACEMENT SHIP SYSTEMATIC SERIES HULL FORMS-SEAKEEPING CHARACTERISTICS

Jan J. Blok and Wim Beukelman

The Society of Naval Architects and Marine Engineers - NO. 4.
Paper to be presented at the Annual Meeting, New York, November 7-10, 1984

Report No. 675-P
Ship Hydromechanics Laboratory - Delft

Delft University of Technology
Ship Hydromechanics Laboratory
Mekelweg 2
2628 CD DELFT
The Netherlands
Phone 015 -786882

THE SOCIETY OF NAVAL ARCHITECTS AND MARINE ENGINEERS
One World Trade Center, Suite 1369, New York, N. Y. 10048
Advance copy of paper to be presented at the Annual Meeting, New York, N. Y., November 7–10, 1984

no. 4

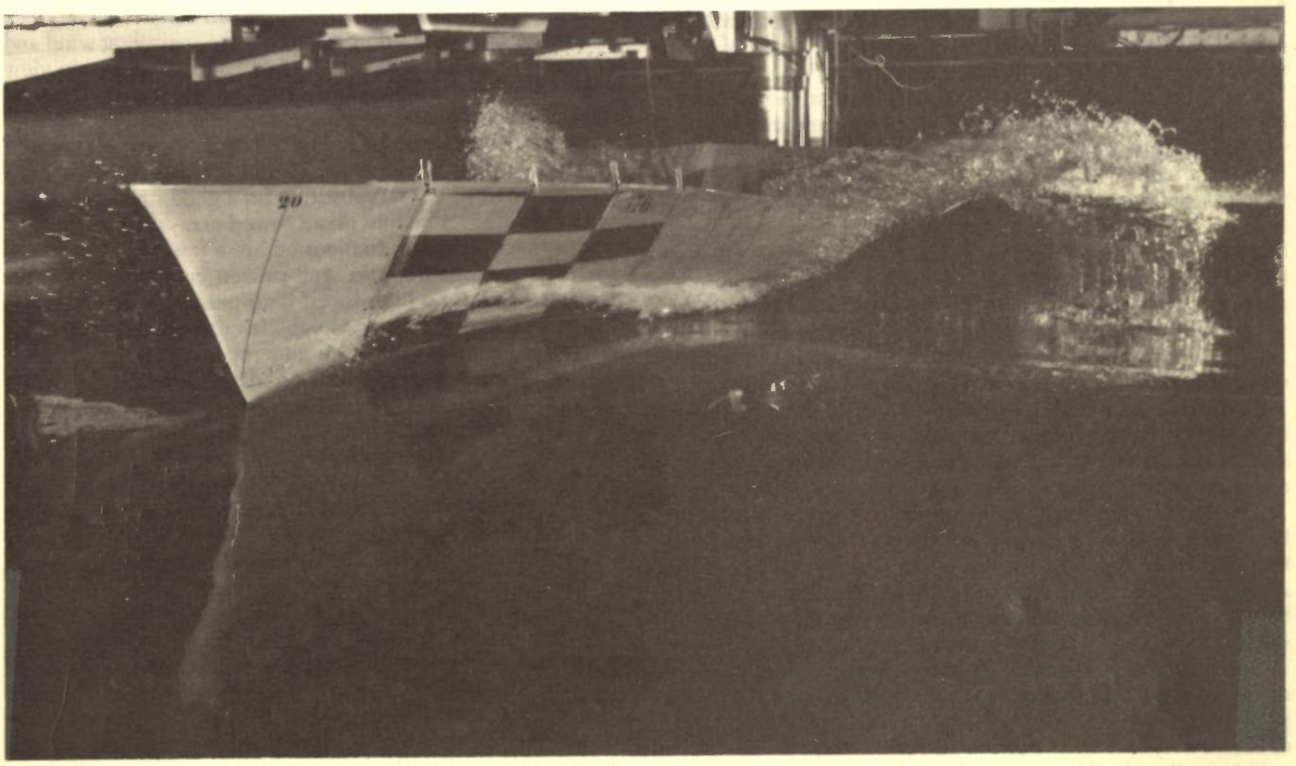

The High-Speed Displacement Ship Systematic Series Hull Forms—Seakeeping Characteristics

Jan J. Blok,[1] Visitor, and **Wim Beukelman,**[2] Visitor

In the operation and design of high-speed ships, a greater emphasis is placed on good seakeeping performance because it is found that large motions and high accelerations can significantly degrade the operational capabilities. The need for better hull forms and the increased interest in seakeeping performance call for more and better data to be available at the design stage to obtain a right balance between seakeeping and other, often conflicting, requirements. In this paper the genesis of a systematic series of model experiments is given, illustrated with results. Attention is focused on the general thoughts underlying the series, the selection of the characteristic section shape, the selection of the basic hull shape, the choice of the parameters to be varied in the series, and the parameters to be fixed from the outset. The choice of the parent hull form and the seakeeping aspects associated with this choice are discussed, and the amalgamation of the data in the form of design charts is shown.

[1] Senior project manager, Ocean Engineering Division, Maritime Research Institute, Wageningen, The Netherlands.
[2] Scientific coordinator, Ship Hydrodynamics Laboratory, Delft University of Technology, Delft, The Netherlands.

For presentation at the Annual Meeting, New York, N. Y., November 7–10, 1984, of THE SOCIETY OF NAVAL ARCHITECTS AND MARINE ENGINEERS.

Introduction

RECENT YEARS have seen an increased interest in seakeeping for naval ships. This has occurred in part because of operators having become aware of significant and quantifiable differences between ships designed for the same task, and in part because researchers have been able to come up with tools to predict ship motions, accelerations and extreme effects and have put together the framework required to estimate the overall performance and its degradation as a result of environmental severity in statistical terms.

In the naval architectural field an inherent assumption is often intuitively made when sufficient data are lacking, that is, "small changes have small consequences." This may be true in many fields of engineering; however, it can prove utterly false in fluid dynamics. The first rule the hydrodynamicist has to learn is that small changes to flow boundary geometry can dramatically alter the flow field [1,2].[3] Ship designers live up to this rule in the design of the underwater hull form inasmuch as they squabble over the lines in a degree unparallelled in any other field of the design.

Seakeeping has long held the stigma of being hard to improve upon and subject to statements like "ships do move anyway." Yet now that the tools, experimental as well as computational, have attained a state of maturity equaling those of other naval architectural fields, it is possible to investigate the seakeeping aspects of a ship at the design stage.

The increased interest in seakeeping for naval ships stems from the full-scale observations, backed up by research findings, that ship's behavior in seakeeping can indeed be improved upon if one is willing to look into it, to handle the elusive tradeoff between uneven and conflicting requirements, and is ultimately willing to pay the price and accept the penalty.

The importance of seakeeping to a naval ship is of a diversified nature. For the ship type we are concerned with in this paper—the fast frigate—seakeeping pervades the operability of almost any system and subsystem of the ship, [3–7].

Ship motions lead to extreme effects like slamming under the bow or green water on deck and attending high loads that can cause damage to the hull and the equipment topside. Excessive motions also lead to substantial weather slowdown or necessitate an unsolicited change of course. Likewise, the motions and attending high accelerations degrade crew performance through restricted movement, increased fatigue and ultimately seasickness [8].

To take but one example, the operation of a helicopter, a feature now to be found on ever smaller frigates and patrol vessels. Ship motions roll and pitch can restrict its on-deck movement; the ship heading relative to the prevailing wind and sea greatly influences its takeoff and landing options in view of the turbulence and exhaust fumes, while the vertical and lateral motions and accelerations at the heli-pad further determine whether it can be recovered or not [9,10]. Although catch-down devices can serve as an expedient to widen the weather window, it is no substitute for a good stable platform. Similar stories can be told about towed arrays and replenishment-at-sea operations, to mention but a few.

Besides the existing and well-proven concept of the displacement hull for a high-speed high-performance platform, a great number of advanced vehicle concepts are under investigation, some of which are more or less actively pursued. We may mention here the advanced displacement-type vessels under which heading we find the "slender ship" concept—essentially a frigate hull of high length-displacement ratio meant to significantly reduce the primary resistance hump. In addition, hulls that hide the greater part of their displacement at a greater depth underwater such as small-waterplane-area single-hull and twin-hull ships (SWASH and SWATH) are thought beneficial in reducing the wavemaking resistance and the motions in a seaway. Semi-planing or fully planing concepts are investigated for ships of limited size and a narrow speed range to reduce resistance. Hydrofoils of various designs have proven their merits and have come into their own as vessels with a high transport efficiency, although still restricted to fair and mildly unfavorable weather. Finally, we may mention air-cushion ships in which high speed and an attractive platform size are combined at the expense of ride quality. All these concepts, and a good deal more that have never left the drawing boards, can operate at high speed and offer an operational advantage of some sort [11–16].

An intriguing question remains as to what limits the true

[3] Numbers in brackets designate References at end of paper.

Nomenclature

a_a = acceleration amplitude (single)
$2\bar{a}_{a1/3}$ = double significant acceleration
a_{19} = acceleration at station 19
B = ship's breadth
b_t = transom stern width
C_A = incremental resistance coefficient for model-ship correlation
C_B = block coefficient
C_{BA} = block coefficient aftbody
C_{BF} = block coefficient forebody
C_{FS} = specific frictional resistance coefficient of ship according to ITTC-57
C_M = midship section coefficient
CG = center of gravity
C_P = horizontal prismatic coefficient
C_{PA} = horizontal prismatic coefficient aftbody
C_{PF} = horizontal prismatic coefficient forebody
C_{RM} = specific residuary resistance coefficient of model
C_{TS} = specific residuary resistance coefficient of ship
C_{VP} = vertical prismatic coefficient
C_{VPA} = vertical prismatic coefficient aftbody
C_{VPF} = vertical prismatic coefficient forebody
C_{WP} = waterplane coefficient
C_{WPA} = waterplane coefficient aftbody
C_{WPF} = waterplane coefficient forebody
F_n = Froude number = $V/\sqrt{g \cdot L}$
$F_{n\nabla}$ = Froude number = $V/\sqrt{g \cdot \nabla^{1/3}}$
g = acceleration due to gravity
i_E = waterline entrance angle relative to centerplane
k = wave number = $2\pi/\lambda$
L = ship's length
L_{PP} = length between perpendiculars
LCB = longitudinal center of buoyancy
LCF = longitudinal center of flotation
Ⓜ = figure of merit according to Bales
rms = root-mean-square value of some quantity
R_{AW} = wave added resistance
R_r = residuary resistance
R_T = total resistance, calm water plus waves
R_{TS} = total resistance in calm water
s_a = relative motion amplitude (single)
s_{17} = relative motion at station 17
T = ship's draft
$\bar{T}_1$ = average wave period
V = speed
V_s = ship speed in knots
z_a = heave amplitude (single)
$2\bar{z}_{a1/3}$ = double significant heave motion
ΔR = wave added resistance
ζ_a = wave amplitude (single)
$\bar{\zeta}_{w1/3}$ = significant wave height
θ_a = pitch amplitude (single)
$2\bar{\theta}_{a1/3}$ = double significant pitch angle
λ = wavelength
∇ = displacement volume
ρ = water mass density
τ = trim angle
ω = wave circular frequency

displacement ship can be pushed and how well she can do at (very) high speed.

In the field of seakeeping these novel concepts have one thing in common: They all perform well provided the sea does not get too rough. The slender ship may exhibit more motions than the usual hulls in a high sea state; the semisubmerged SWASH and SWATH rely heavily on their control flaps for good performance; planing hulls just do not perform in waves, while hydrofoils whether they cut through the wave crests or contour the waves have a limit on sea state above which they simply cannot be operated or have to go down to the hull-borne mode. Finally, air-cushion ships: Although the ride comfort will be dramatically reduced in waves, it is doubtful if the cushion can be maintained at all in a severe sea state [11,12].

Studies on novel ship types that come into the picture for naval applications have shown that the order of importance to be attached to the various disciplines is seakeeping first, then stability and control both in the vertical plane and in maneuvering, further propulsion hydrodynamics, and finally resistance. This sequence of importance is quite unlike the order usually adhered to in displacement hull design, where perhaps the order should also be reversed.

In the foregoing we have identified the need for seakeeping data to be available as early as possible in the design stage of a high-speed combatant in order to get the maximum out of it. In addition, the oncoming novel hull concepts force us to face the question, "How good can displacement hull forms perform at high speed?" For both of these reasons a systematic series of model experiments has been initiated to produce calm-water resistance data and motion, acceleration, and added drag data in waves for an extensive series of displacement hull forms.

The hull forms were to be applicable to 15-m (50 ft) patrol craft and up to 150-m (500 ft) cruisers alike, and the speed range sufficient to embrace the highest speeds envisaged for the novel hull concepts, that is, Froude numbers of well over unity (metric, dimensionless). It was further meant to design the hull forms in a coherent fashion so that a true family of models would emerge, and to present the data in a form of design charts amenable to quick estimation of salient characteristics. Various apects of the series are discussed herein, mainly with a view to seakeeping.

The choice of the parameters was an important point, which to keep fixed and which to vary, and the resulting parameter space is illustrated. Further, a tradeoff was to be made between stillwater resistance and seakeeping in the selection of the characteristic section shape and the characteristic hull shape. Moreover, the reasoning and deliberations that led to the selection of the parent hull form are given. Experimental setup and test program are subjects discussed in some detail and typical results are given.

In addition to the model experiments, a series of computations was made with strip theory programs and correlated with the measurements to determine to what extent existing analytical tools can predict the performance of ships in a speed range hitherto not included. Finally, a prediction is shown for a typical 85-m (280 ft) frigate on the basis of the series data.

Setting up the systematic series

In the design of the series a number of aspects had to be considered in detail. Among these were the design criteria for the series, its speed range, the appropriate parameters, and the parent hull form selection. We will touch upon these in the following.

Design criteria

In setting up the series it was important to adopt design criteria first. A systematic series hinges on the choice of the characteristic hull shape—the parent hull—which can be selected only in the light of a set of design criteria. Furthermore, for the scope of the series and its parameter selection and parameter space as well as the subsequent test program details, a set of design criteria would be an imperative departure point. The criteria formulated for this hull-form series were:

- good calm-water resistance properties, and
- good seakeeping characteristics.

Concerning the first point, attention focused on resistance; for the time being, propulsion was left out of the picture. The second point, seakeeping, was elaborated to cover

- low motion and acceleration levels,
- low wave added resistance, and
- small probability of incurring extreme effects like slamming under the bow and shipping of water on deck.

These criteria can all be narrowed down to one and the same—low motion levels—because usually if the motions decrease, the accelerations and the wave added drag will also go down. Extreme effects may not always follow suit, but can be remedied easily by ensuring a sufficient draft forward and an appreciable freeboard and flare on the forebody.

For the subject high-speed ships it was further considered that the most critical motion and acceleration levels would occur in head seas. Wave added resistance is also largest in that case. It goes without saying that other wave headings may pose other problems on the ship; for instance, rolling in beam seas and in stern quartering seas. For the purpose of comparison of hull forms, however, it was deemed sufficient to study the hulls only in head seas. The restriction following from this design requirement has to be imposed on the series before the relevant parameters are selected.

Speed range of interest

The two aims of the study, namely to generate data of use to the designer and to investigate what the limits are of the displacement hull, necessitated a wide speed range for the series.

Patrol craft of small displacement encounter very high Froude numbers,[4] which may easily get as high as $F_n = 1.2$, while the intermediate range around $F_n = 0.7$ is of interest for frigates of the usual size, $L = 120$ m (400 ft), when pushed up to 45 knots. In addition, however, most navies express a great interest in the cruising speed range of 15 to 25 knots for reasons of peacetime fuel economy, for all ship types and sizes.

Consequently it was decided that for the present series to be of any great value and to meet the aims an extremely wide speed range had to be adopted ranging from $F_n = 0.1$ to 1.2.

For the selection of the parent form a hull would have to be selected that would be optimum preferably over the whole speed range. If a tradeoff should be encountered, the speed range of $F_n = 0.7$ to 1.0 would have the emphasis.

Parameters of interest

In the design of the systematic series a set of parameters had to be identified that would have a bearing on stillwater resistance and seakeeping performance alike. A second and by no means less essential requirement was that the parameters be of practical significance to the ship designer. A third point lay in the fact that we are dealing with ship forms rather than dimensional ships, so that the parameters to be selected had to be nondimensional quantities. Bearing this in mind and keeping

[4] In the text two Froude numbers are used, one based on the ship length, the other based on the third root of the displacement. Because of the use of the acceleration due to gravity and metric units, both expressions are dimensionless: $F_n = V/\sqrt{g \cdot L}$ and $F_{n\nabla} = V/\sqrt{g \cdot \nabla^{1/3}}$.

Table 1 Main parameters

L/B, B/T	L/T	$L/\nabla^{1/3}$
C_P, C_B	C_M	
C_{VP}	C_{WP}	
LCB, LCF	LCB – LCF separation	
b_t/B	(transom width over ship's breadth)	
i_E	(waterline entrance angle)	

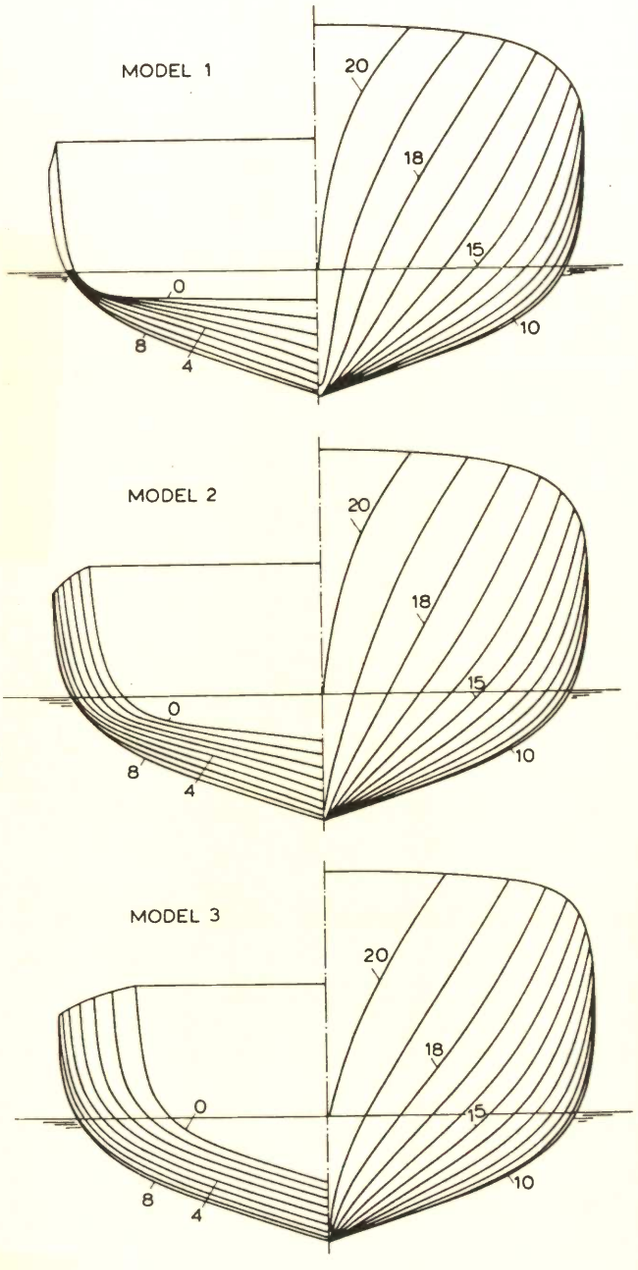

Fig. 1 Body plans of models

an eye on the design criteria, a number of main parameters were selected as listed in Table 1.

It will be obvious that if all of these are varied over only two values, independently from the others, a prohibitively large number of models would result, and it is even questionable if all of them would be really independent of one another if one wants to avoid odd shapes. Therefore, a number of parameters have to be fixed and only a limited number will come in for variation.

Parameters to be fixed and varied

To reduce the number of models and to adhere to parameters of direct interest to the designer, it was decided to take the L/B, B/T, and C_B coefficients as prime parameter to be varied in the series and to fix all others as optimal as could be established for the parent hull.

The choice of these three parameters is certainly justified from the stillwater resistance and from the seakeeping point of view. Along with the variation of these parameters a number of other parameters vary as well; L/T, $L/\nabla^{1/3}$, C_P, C_M, C_{WP}, or C_{VP}; so the choice is not too restrictive.

The prime parameters L/B and C_B have a decided influence on stillwater resistance as have the secondary variables $L/\nabla^{1/3}$, C_P, and C_M. The prime variable B/T and the secondary variables L/T, C_{WP}, and C_{VP} have a profound influence on seakeeping.

So, it will be clear that the selection of only these three parameters, which will come in useful from the designer's angle, is by no means a restriction from the hydrodynamic point of view.

Subseries 1

It follows as a logical consequence from the foregoing that a limited number of parameters will have to be fixed from the outset:

C_P
C_{WP} or C_{VP}
LCB
LCF
b_t/B
i_E

It was felt that sufficient information was available to accurately determine the optimum value of LCB and b_t/B. See for instance Bailey [17], who presented results on the effect of systematic variation of LCB on calm-water resistance, indicating a foremost limit on LCB of 6.2 percent of L abaft the midships. As to the choice of LCB, a constant position of 5 percent abaft the midships was chosen as it was shown in the Maritime Research Institute Netherlands (MARIN) data set to be an optimum value for the majority of cases.

The optimum value of C_P could be estimated quite well from the extensive data set on existing ships, while the same applied to i_E. The C_P values adopted for other systematic high-speed hull form series were: Series 64 by Yeh [18], $C_P = 0.63$; Lindgren and Williams series [19], $C_P = 0.68$; and the National Physical Laboratory (NPL) series by Bailey [17], $C_P = 0.693$. For the high-speed hulls in the MARIN data set a clear correlation existed between C_B and C_M so that C_P was chosen at a fixed value, $C_P = 0.63$, for all block coefficients (see Fig. 8).

Little systematic work has been done on seakeeping, certainly not at $F_n = 1$, so less certainty existed as to the choice of LCF, which was thought to have a marked influence on seakeeping. The decision was taken to devote a short subseries of three models to determine the optimum value of LCF within certain bounds, that is, between 6 and 9 percent aft of midships. For this reason three models were designed having the same curve of sectional areas, varying LCF, and of necessity also different

C_{WP} and C_{VP}. The resulting body plans of these three models, Fig. 1, show that for the same displacement and in fact on the same curve of sectional areas a gradual transition was made from a narrow-forebody/wide-aftbody shape (Model 1) to a wide-forebody/narrow-aftbody shape (Model 3). In order to keep to realistic models it was felt that for this great a shift in LCF, it was not entirely possible to keep C_{WP} the same. We would have liked to, but the waterplane width forward would have been too much and the waterline entrance angle would have become too large for Model 3. Therefore, of necessity, C_{WP} was reduced from Model 1 to Model 3 and C_{VP} likewise went up for the same C_B; see Fig. 2. As a consequence, the results to be found from these models, perhaps not so much on resistance, but all the more so on seakeeping, cannot be attributed to LCF only. Yet the differences in seakeeping between the three models, if only attributed to narrow-wide and wide-narrow configurations, are unmistaken.

This was perhaps one of those points in which "scientific rigor" (whatever that may be), or the wish to vary only one parameter at a time, which is elegant when dealing with systematic series, had to give way to the one and only rule that pervades this whole series, "the hull forms have to be realistic and practical."

When the results on these three models became available and were collated with other data, it was found that still more improvements could be made. Therefore the models were cut up amidships and the fore and aft bodies combined in a different way. This resulted in models with a wider waterplane area for the same displacement. Three models thus obtained, denoted Models 4, 5, and 6, were also tested. Figure 3 gives

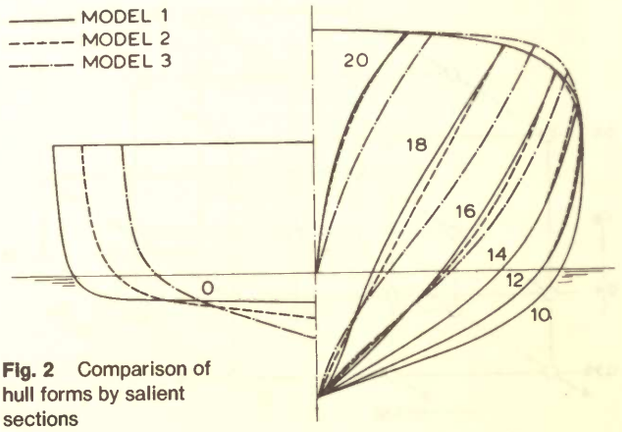

Fig. 2 Comparison of hull forms by salient sections

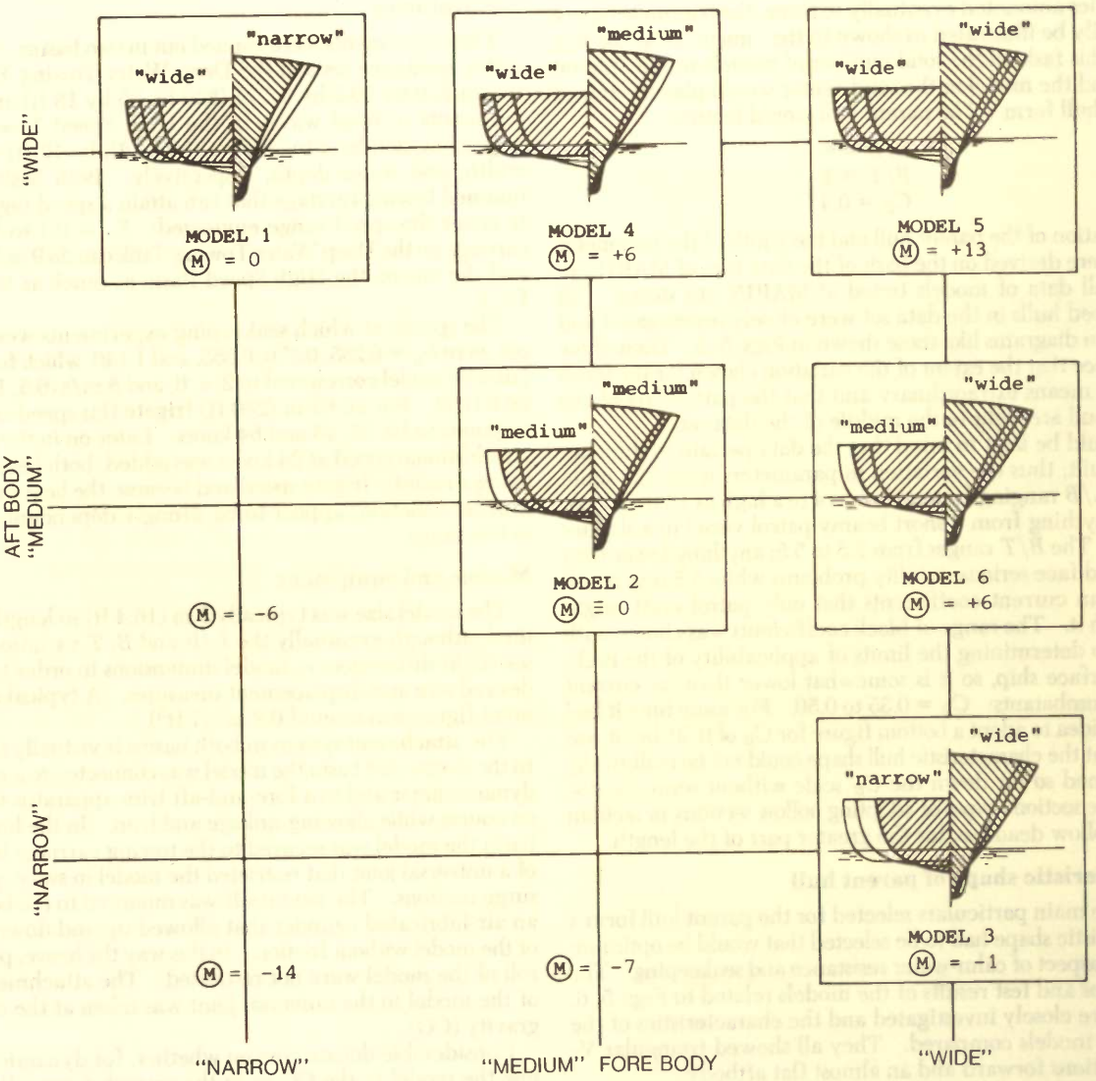

Fig. 3 Models tested

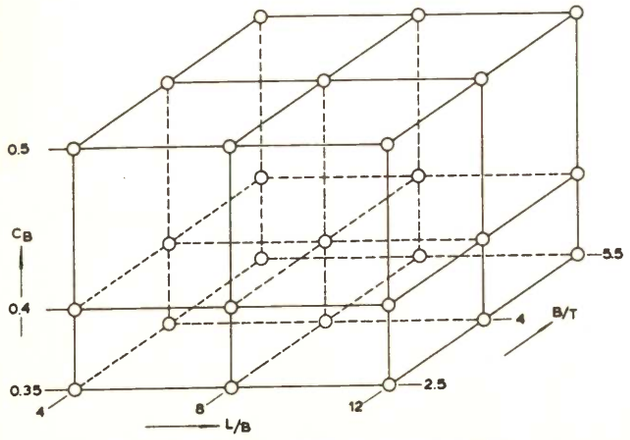

Fig. 4 Parameter space for entire test series

a quick-look impression of how the six models are related to one another.

Parameter space of entire series

Because the total number of parameters to be varied in the true series amounted eventually to three, the parameter space can easily be illustrated as shown in the "magic cube" of Fig. 4. In this fashion the total number of models would amount to 27 and the model in the solid center would play the role of parent hull form. The parent hull would feature:

$$L/B = 8$$
$$B/T = 4$$
$$C_B = 0.4$$

The location of the parent hull and the width of the parameter space were derived on the basis of the data files of MARIN, in which all data of models tested at MARIN are stored. All high-speed hulls in the data set were closely investigated and plotted in diagrams like those shown in Figs. 5–8. These show at a glance that the extent of the variation chosen for the series is by no means extraordinary and that the particulars of the parent hull are right in the middle of the data set.

It should be kept in mind that the data pertain to ships actually built; thus the variation in parameters would be quite wide. L/B ranging from as low as 4 to a high as 12 should include anything from a short beamy patrol vessel to a slender cruiser. The B/T ranges from 2.5 to 5.5; anything lower than 2.5 would face serious stability problems while 5.5 is so much more than current coefficients that only patrol craft might approach it. The range of block coefficients was chosen with an eye to determining the limits of applicability of the high-speed surface ship, so it is somewhat lower than for current surface combatants: $C_B = 0.35$ to 0.50. For some time it had been the idea to adopt a bottom figure for C_B of 0.30, but it was found that the characteristic hull shape could not be realistically transformed so far down the C_B scale without seriously distorting the section shapes or adopting hollow sections, or sections with a hollow deadrise, for the greater part of the length.

Characteristic shape of parent hull

For the main particulars selected for the parent hull form a characteristic shape had to be selected that would be optimum from the aspect of calm-water resistance and seakeeping. The body plans and test results of the models related to Figs. 5, 6, and 7 were closely investigated and the characteristics of the very best models compared. They all showed triangular V-shape sections forward and an almost flat aftbody.

Most of them were round bilge, some of them were hard-chine forms. For the characteristic form of the series a round bilge was adopted as it was felt that hard-chine forms, even when optimum for the parent, might not be optimum for the transformed shapes. Moreover, hard chines have their benefit in the planing or semiplaning mode, which comes about only at speeds $F_n > 1.2$—on the verge of the present series. In addition, the series was intended to be for true displacement hulls with perhaps some dynamic lift from planing, but not more than say 10 percent at the highest speed.

The characteristic shape first drawn up is shown as Model 2 in Fig. 1. The transom stern does not extend over the full width of the beam, and the forward sections at least for the forward quarter ship length are truly triangular. It should be well understood that the characteristic shape—the parent hull—emerged as the condensate of a great number of one-off designs that were all extensively tested and modified to get the maximum out of them and that have actually been built.

Experimental program

For the most part the research program on systematic hulls is an experimental program, the experiments being done in various basins and in still water and in waves. The general approach and some interesting details follow.

Laboratories

The experiments were carried out in two basins: the calm-water resistance tests in the Deep Water Towing Tank measuring 250 by 10.5 by 5.5 m (820 by 35 by 18 ft) and the experiments in head waves in the High Speed Towing Tank measuring 220 by 4 by 3.6 m (720 by 13 by 12 ft) in length, width, and water depth, respectively. Both basins have a manned towing carriage that can attain a speed high enough to cover the speed range envisaged: $F_n = 0.1$ to 1.2. The carriage on the Deep Water Towing Tank can do 9 m/s (30 ft/s) and the one on the High Speed Basin as much as 15 m/s (50 ft/s).

The speeds at which seakeeping experiments were carried out were $F_n = 0.285$, 0.570, 0.855, and 1.140, which for the 5-m (16.4 ft) model correspond to 2, 4, 6, and 8 m/s (6.5, 13.1, 19.7, 26.2 ft/s). For an 85-m (280 ft) frigate this speed range corresponds to 16, 32, 48 and 64 knots. Later on in the program an additional speed at 24 knots was added, both because of its being a realistic frigate speed and because the heave and pitch transfer functions appear to be strongly dependent on speed in this range.

Models and equipment

The model size was typically 5 m (16.4 ft) in length (waterline) although eventually the L/B and B/T variations would see slight differences in model dimensions in order to keep to desired size and displacement measures. A typical displacement figure was around 0.2 m^3 (7 ft^3).

The attachment system in both basins is virtually the same. In the deepwater basin the model was connected to a resistance dynamometer and to a fore-and-aft trim apparatus to keep it on course while allowing sinkage and trim. In the high-speed basin the model was secured to the towing carriage by means of a universal joint that restricted the model in sway, yaw, and surge motions. The joint itself was mounted to the bottom of an air-lubricated cylinder that allowed up and down motion of the model without friction. In this way the heave, pitch, and roll of the model were not restricted. The attachment point of the model to the universal joint was taken at the center of gravity (CG).

Considerable debate goes on whether, for dynamic tests, to tow the model in the CG or in the extended propeller shaft. Since neither of the two were known quantities in this series,

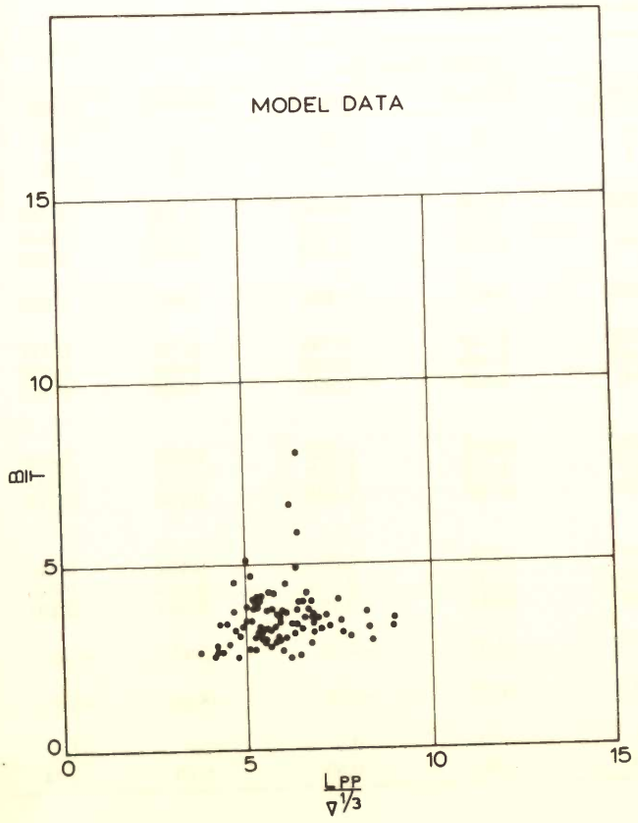

Fig. 5 Correlation of B/T to $L/\nabla^{1/3}$

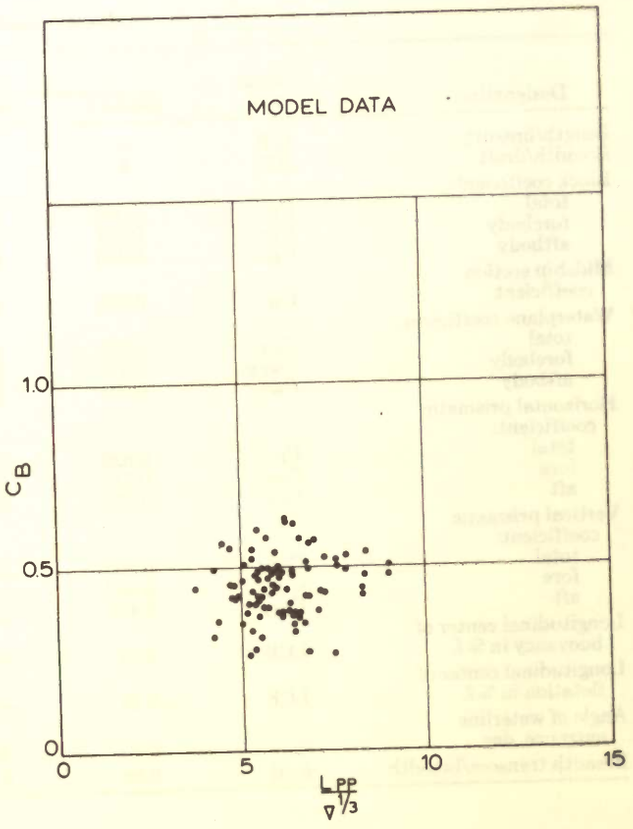

Fig. 7 Correlation of C_B to $L/\nabla^{1/3}$

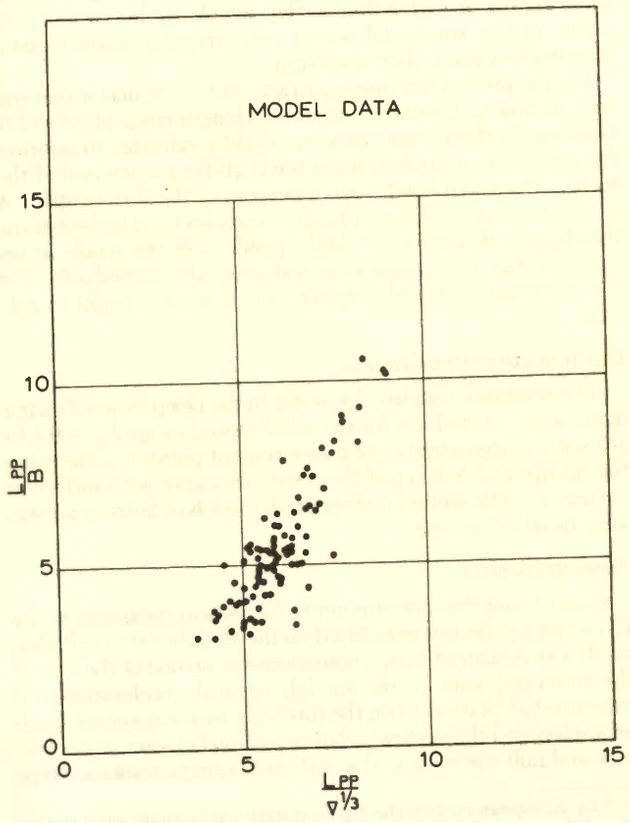

Fig. 6 Correlation of L/B to $L/\nabla^{1/3}$

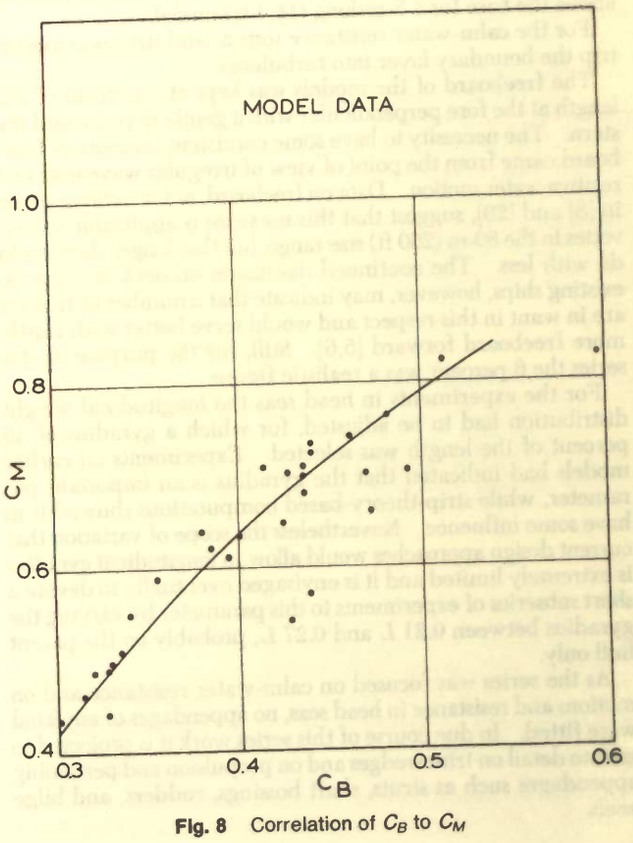

Fig. 8 Correlation of C_B to C_M

Table 2 Coefficients of the models

Designation	Notation	NSMB Model No. Model 1	Model 2	Model 3	Model 4	Model 5	Model 6
Length/breadth	L/B	8	8	8	8	8	8
Breadth/draft	B/T	4	4	4	4	4	4
Block coefficient:							
total	C_B	0.396	0.396	0.396	0.396	0.396	0.396
forebody	C_{BF}	0.327	0.327	0.327	0.327	0.327	0.327
aftbody	C_{BA}	0.465	0.465	0.465	0.465	0.465	0.465
Midship section coefficient	C_M	0.633	0.633	0.633	0.633	0.633	0.633
Waterplane coefficient:							
total	C_{WP}	0.785	0.768	0.749	0.790	0.796	0.774
forebody	C_{WPF}	0.577	0.588	0.600	0.588	0.600	0.600
aftbody	C_{WPA}	0.992	0.947	0.898	0.992	0.992	0.947
Horizontal prismatic coefficient:							
total	C_P	0.626	0.626	0.626	0.626	0.626	0.626
fore	C_{PF}	0.517	0.517	0.517	0.517	0.517	0.517
aft	C_{PA}	0.735	0.735	0.735	0.735	0.735	0.735
Vertical prismatic coefficient:							
total	C_{VP}	0.505	0.516	0.528	0.501	0.497	0.512
fore	C_{VPF}	0.567	0.556	0.545	0.556	0.545	0.545
aft	C_{VPA}	0.469	0.491	0.518	0.469	0.469	0.491
Longitudinal center of buoyancy in % L	LCB	−4.97	−5.12	−5.16	−5.02	−5.11	−5.22
Longitudinal center of flotation in % L	LCF	−9.23	−8.11	−6.77	−9.01	−8.68	−7.77
Angle of waterline entrance, deg	i_E	6.5	9.5	11.0	9.5	11.0	11.0
Breadth transom/breadth	b_t/B	0.89	0.74	0.59	0.89	0.89	0.74

a decision was taken to select one point which would be held constant for all models. The CG was chosen at 60 percent of the depth of the model, which worked out at 0.169 m (0.55 ft) above the base for a 5-m-long (16.4 ft) model.

For the calm-water resistance tests a sand strip was used to trip the boundary layer into turbulence.

The freeboard of the models was kept at 6 percent of the length at the fore perpendicular with a gentle slope toward the stern. The necessity to have some consistent measure of freeboard came from the point of view of irregular wave tests and relative water motion. Data on freeboard, as for instance given in [3] and [20], suggest that this measure is applicable to corvettes in the 80-m (260 ft) size range, but that longer ships could do with less. The continued discussion on deck wetness on existing ships, however, may indicate that a number of frigates are in want in this respect and would serve better with a little more freeboard forward [5,6]. Still, for the purpose of this series the 6 percent was a realistic figure.

For the experiments in head seas the longitudinal weight distribution had to be adjusted, for which a gyradius of 25 percent of the length was selected. Experiments on earlier models had indicated that the gyradius is an important parameter, while strip-theory-based computations showed it to have some influence. Nevertheless the scope of variation that current design approaches would allow in longitudinal gyradius is extremely limited and it is envisaged eventually to devote a short subseries of experiments to this parameter by varying the gyradius between 0.21 L and 0.27 L, probably on the parent hull only.

As the series was focused on calm-water resistance and on motions and resistance in head seas, no appendages of any kind were fitted. In due course of this series work it is projected to go into detail on trim wedges and on propulsion and pertaining appendages such as struts, shaft bossings, rudders, and bilge keels.

Regular-wave and irregular-wave experiments

The High Speed Towing Tank has a hydraulically operated wave generator with a double flap which can be used to generate regular sinusoidal waves and irregular seaways conforming to a prescribed spectrum.

For the present test program a series of 11 regular waves was used, spanning the wavelength to ship length range of 0.6 to 2.8. Later on the short wave range was slightly extended to improve the acceleration prediction on the high-frequency end of the scale. The wave height was 2 percent of the ship length. A series of waves at different heights was also tried to determine the degree of linearity at high speed. For the whole series shown in Fig. 4, irregular wave tests were also carried out. For the subseries of models, regular waves were thought to suffice.

Calm-water experiments

The resistance tests in calm water in the Deep Water Towing Tank were carried out for the whole speed range $F_n = 0.1$ to 1.2 with a large number of measurement points to determine the humps and hollows of the resistance curve with sufficient accuracy. The wetted surface of all models of Subseries 1 was very nearly the same.

Measurements

Concerning the measurements, heave was measured at the CG using a potentiometer fitted on the air-lubricated cylinder; pitch was measured with a potentiometer on one of the axes of the universal joint in the model; vertical acceleration was measured at [5]station 19 on the forebody by means of an accelerometer; and the vertical relative motion between water surface and hull was measured at station 17 using a resistance-type

[5] By European custom the transom stern has been denoted station 0 and the fore perpendicular station 20.

wave probe. The model resistance was recorded in a strain-gage cell in the universal joint so that the resistance force measured remained horizontal at all times.

For the correction of the phase angles to the wave crest it was necessary to have a measure of the wave; this was taken 3.5 m (11.5 ft) ahead of the model. As the very high speed would render ordinary wave probes useless because of the wave system of the wires themselves, a servo-controlled wave follower device was used that could cope with the very high velocities and accelerations.

Measurements were all recorded on fiber optics recorder strip charts for quick-look inspection and on magnetic tape for proper analysis.

Results on seakeeping behavior

From the wealth of data obtained from the experiments the most salient results are shown in the paper. The results are exclusively related to the forerunner series of models shown in Fig. 3 that led to the choice of the parent hull in the solid centre of the cube in Fig. 4; see also Table 2.

Influence of geometry on heave

Figures 9–12 serve to illustrate the influence of model geometry on characteristic seakeeping transfer functions for one speed, $F_n = 0.570$. In Fig. 9 for heave the differences between the models amount to some 10 percent in the region of wavelength, which is of most interest to this kind of ship at such speeds. It is not possible to attribute the differences to one single cause, as many influence factors change.

The wave exciting force for heave is directly proportional to the waterplane area, which was different for all six models. The one with the largest waterplane area, Model 5 ($C_{WP} = 0.796$), would have the largest wave exciting force. The added mass is to leading order proportional to beam squared, then to B/T ratio, and finally to section shape. Model 5 would also have the largest added mass, which would suppress the motions in the high-frequency regime.

As to the damping, also proportional to beam squared, the same can be said, and it may be expected that the model with the largest C_{WP} (No. 5) would have the highest damping and the lowest transfer function in the $\lambda/L = 1$ region. The difference in spring rate is proportional to the waterplane area, hence the C_{WP}, and in the long wave range the model with the largest C_{WP} would have the lowest transfer function in heave. The differences due to change in heave-pitch coupling can be understood only through a direct computation, for instance with strip theory. With the foregoing in mind the qualitative trend of the data in Figs. 9–12 can be explained to a fair degree.

Model 5 has the largest C_{WP} and thus the greatest waterplane area for the same displacement, resulting in very low heaving for all speeds. Model 3 has the lowest C_{WP} and thus the smallest waterplane area for the same displacement, resulting in rather large heave motions for most speeds. Because the block coefficient is kept constant, the heave motion exhibits the same trend on the basis of $(C_{VP})^{-1}$. The differences in heave between the six models are largest around $\lambda/L = 1.2$ for low speed and around $\lambda/L = 2.4$ for the highest speed, which demonstrates that the greatest differences are to be found around the peak of the magnification factor z_a/ζ_a. The influence of C_{VP} on heave will be noted in Fig. 9; it is even more pronounced for higher speeds where it is found that the models with the lowest C_{VP} (Models 1, 4, and 5) have the smallest heave, whereas the other three with the highest C_{VP} have the greatest heave. Because of other effects such as LCB-LCF separation, which greatly influences the heave-pitch coupling, the heaving may not always be directly in line with the C_{VP}, but a strong dependency certainly exists in this case. When we relate C_{VP} to hull shape we find that for this family of models the great breadth of the transom stern, and as a direct result the width of the whole aftbody, is of direct influence on C_{VP}, so that we may qualitatively conclude that a wide aftbody results in a high C_{VP}, which in turn results in low heaving. This reasoning cannot be detached from the present family of models in which the displacement and the block coefficient were kept the same, and in which the C_{WPF} was not allowed to vary to the same extent as C_{WPA} because the waterline entrance angle had to remain fine.

Influence of geometry on pitch

When we take a look at the pitch functions of all six models, shown in Fig. 14, we find a 10 percent difference mainly around resonance (where it matters). Since pitching is the most dominant motion in head seas, it may be better to take a look at Figs. 13 to 16, where the pitch functions are shown for all six models and for all four speeds. Where the differences at low speed amount to some 10 percent, the differences at high speed are by no means marginal, but amount to some 45 percent in the λ/L range around 2.2. These figures show a striking trend. If the models are again ranked on the basis of their C_{VP}, it is found (Fig. 16) that the model with the lowest C_{VP} exhibits the smallest pitch angle. As the C_{VP} increases, the pitch angle goes up, almost proportionally. For the highest speed, $F_n = 1.14$, this comes out beautifully; for the lower speed, the differences are not so large but the same trend still exists. No such clear-cut trend can be established on the basis of LCB or LCF or their separation, so that the conclusion seems warranted that a low C_{VP} brings about a small pitch angle, regardless of the LCB-LCF separation. One should, however, be careful about taking this conclusion outside the present family of models.

Influence of geometry on accelerations

The vertical acceleration at station 19, shown in Fig. 11, is for head seas essentially the result of combined heaving and pitching, and likewise bears a linear relationship to the wave amplitude. In order to adhere to the Froude scaling law and to make the acceleration nondimensional in the transfer function, the acceleration has been divided by ζ_a/L, the ratio between wave amplitude and model length. Although in the present case the accelerations were actually measured, they might just as well have been calculated from heave and pitch and their relative phase angles. When we compare this Fig. 11 to the pitch function in Fig. 14, we find the same trend on the basis of model geometry. The model with lowest C_{VP} produces the lowest acceleration and, as the C_{VP} goes up, the vertical acceleration at synchronous pitching goes up as well. It shows, at least for this speed, that a number of models virtually coincide as to their acceleration levels, but for other speeds this is not the case.

Relative motions

The relative motion between hull and water surface was recorded only at station 17; this was done with wires flush with the hull. Because of the problem of how to define exactly what one is measuring in this way—spray; solid water jetted upward and a sheet of water creeping upward all have their influence on the electronic measurement—this measurement should be regarded as indicative, certainly at the highest speed where spray was very much in evidence. Much the same, the concept of relative motion being the result of combined heaving, pitching and incident waves becomes questionable; water particles touching the stem at the waterline level will be flying past station 17 a little higher up and may wet the deck at station 10. Concerning the shape of the transfer function there exists a close correspondence between the pitch function and the acceleration function.

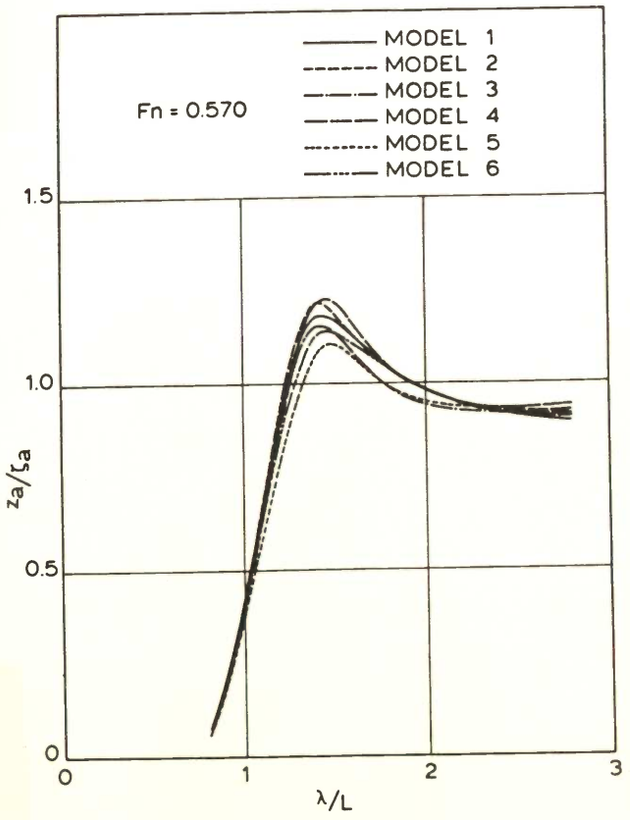

Fig. 9 Heave transfer functions

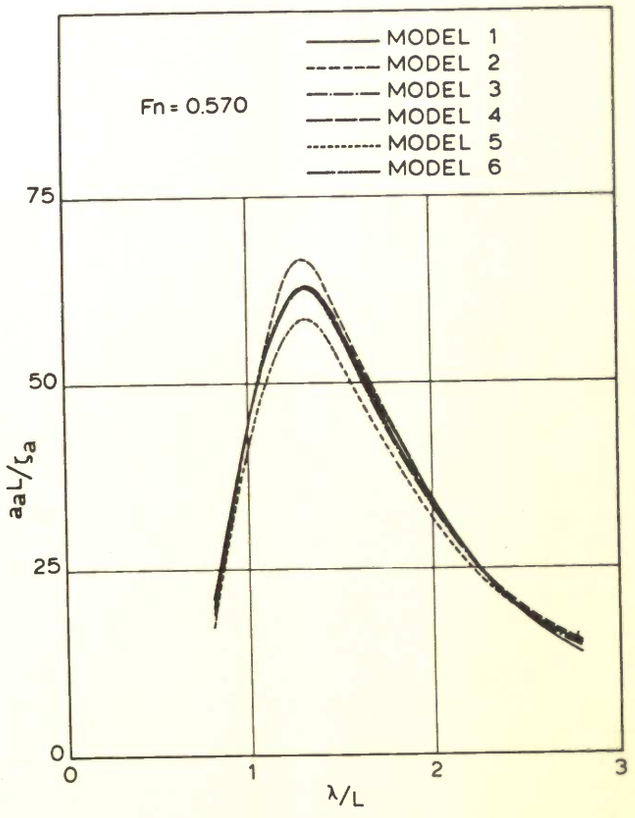

Fig. 11 Vertical acceleration transfer functions

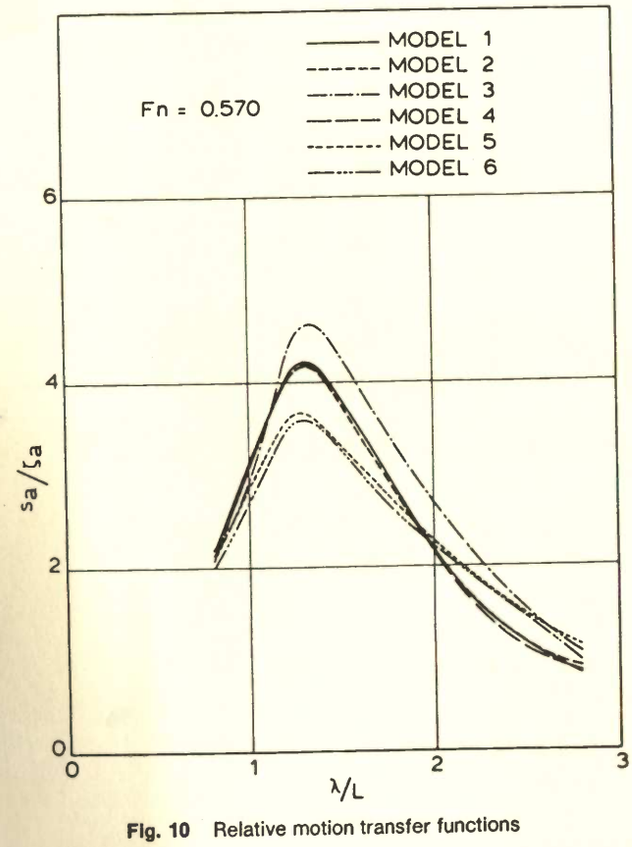

Fig. 10 Relative motion transfer functions

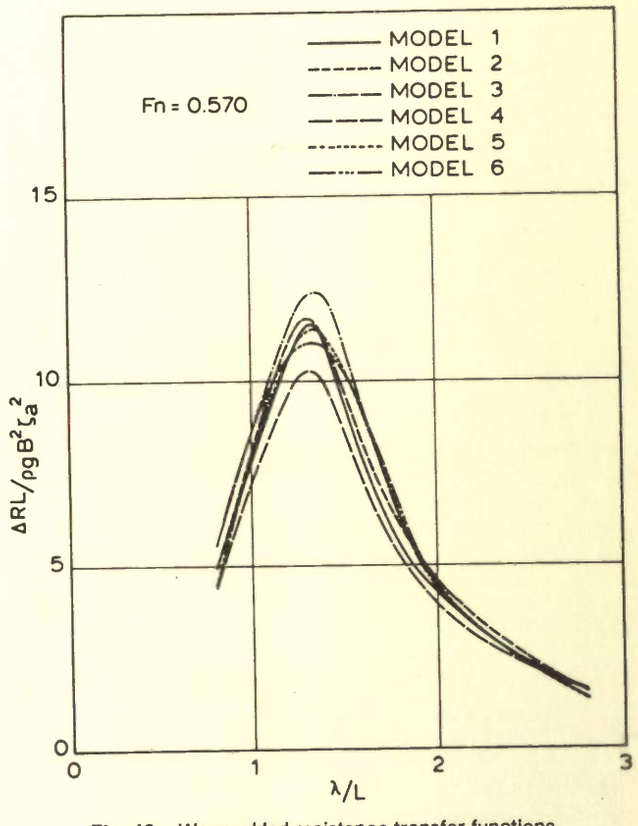

Fig. 12 Wave added resistance transfer functions

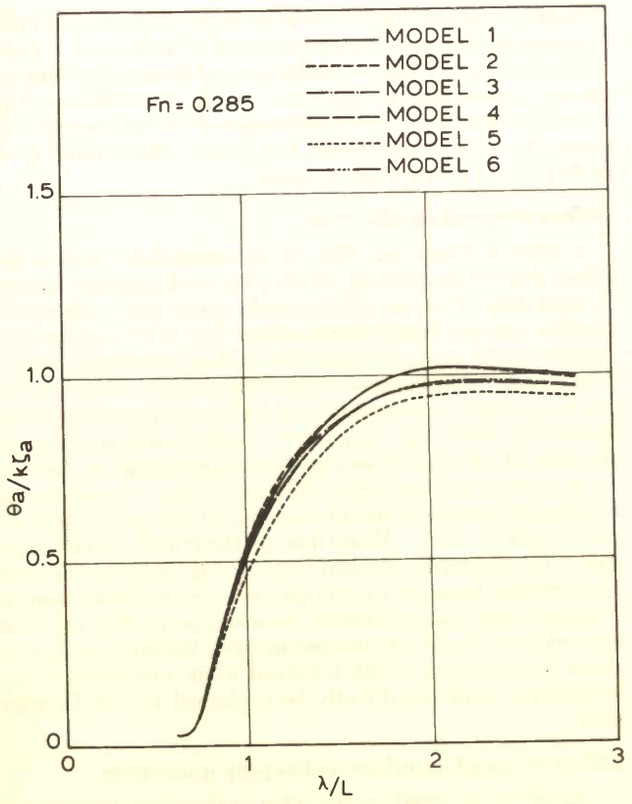

Fig. 13 Pitch transfer functions

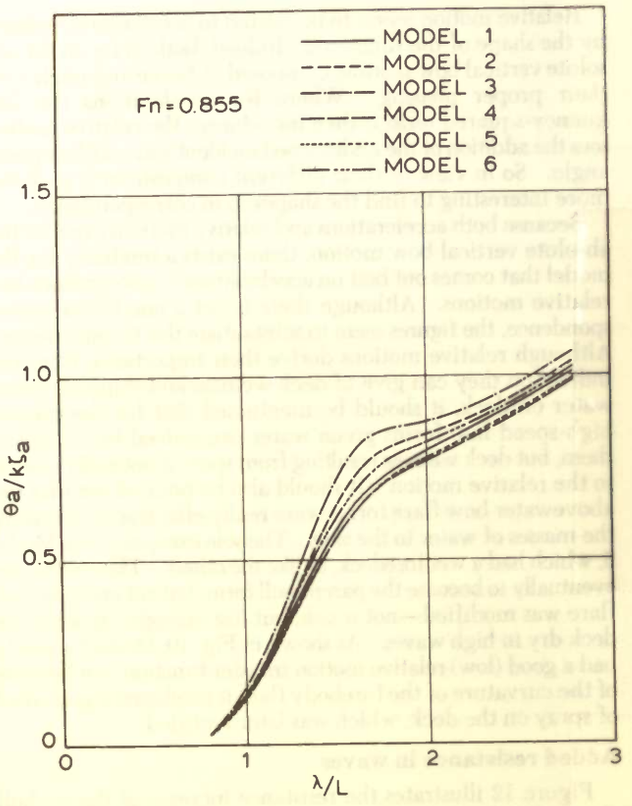

Fig. 15 Pitch transfer functions

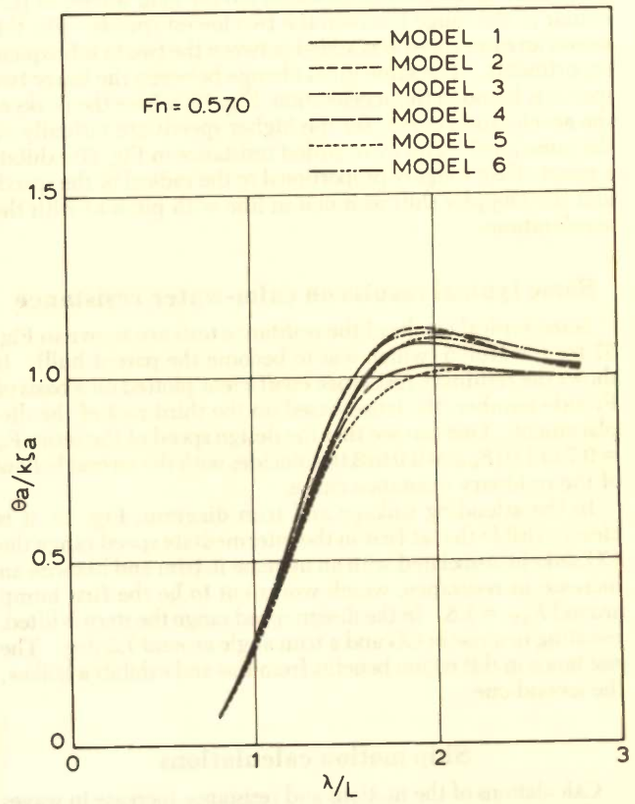

Fig. 14 Pitch transfer functions

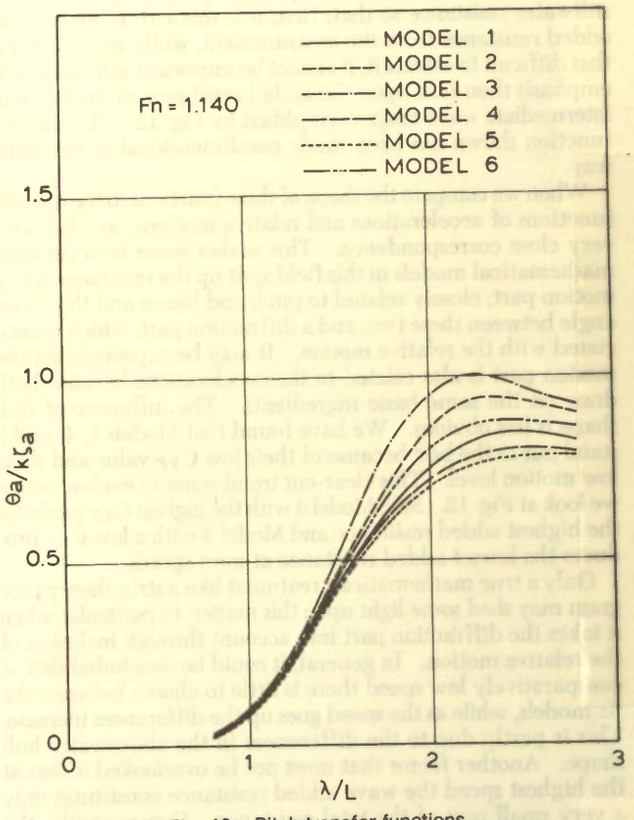

Fig. 16 Pitch transfer functions

Relative motion seems to be related to acceleration, judging by the shape of the functions. Indeed, both draw on the absolute vertical bow motion, composed of heave and pitch with their proper phasing. Where for accelerations the frequency-squared term is then introduced, the relative motion sees the addition of the undisturbed incident wave with its phase angle. So in view of their different composition it is all the more interesting to find the shapes so in correspondence.

Because both accelerations and relative motions draw on the absolute vertical bow motion, there exists a tendency for the model that comes out best on accelerations to also produce low relative motions. Although there is not a one-to-one correspondence, the figures seem to substantiate this to some degree. Although relative motions derive their importance from the indication they can give of deck wetness and shipping green water on deck, it should be mentioned that for the present high-speed hull forms green water can indeed be related to them, but deck wetness resulting from spray is not easily related to the relative motion. It should also be pointed out that the abovewater bow flare forms were really effective in throwing the masses of water to the side. The sole exception was Model 5, which had a wet foredeck, unlike the others. This model was eventually to become the parent hull form, but not until the bow flare was modified—not much, but just enough—to keep the deck dry in high waves. As shown in Fig. 10, Model 5 already had a good (low) relative motion transfer function, but because of the curvature of the forebody flare it produced a good deal of spray on the deck, which was later rectified.

Added resistance in waves

Figure 12 illustrates the resistance increase of the six hull shapes. It should be borne in mind that as the speed goes up, the stillwater resistance increases with the square of the speed. The wave added resistance shows some speed effect but this can hardly be expressed as a power function. So, at high speed the added resistance becomes comparatively small relative to the stillwater resistance so that, first, it is difficult to extract the added resistance from the measurement, while second, if it is that difficult to extract it, it cannot be important after all. The emphasis then falls upon the added resistance in the low and intermediate wave range exemplified by Fig. 12. The transfer function shown has been made nondimensional in the usual way.

When we compare the shape of these functions to the transfer functions of accelerations and relative motions, we observe a very close correspondence. This makes sense because most mathematical models in this field split up the resistance into a motion part, closely related to pitch and heave and the phase angle between these two, and a diffraction part, which is associated with the relative motion. It may be expected that the motion part is also related to the accelerations because both draw on the same basic ingredients. The influence of hull shape is less obvious. We have found that Models 1, 4, and 5 stand out as the best because of their low C_{VP} value and their low motion level. This clear-cut trend is not so evident when we look at Fig. 12. Still, Model 3 with the highest C_{VP} produces the highest added resistance and Model 4 with a low C_{VP} produces the lowest added resistance at most speeds.

Only a true mathematical treatment like a strip theory program may shed some light upon this matter, in particular when it takes the diffraction part into account through inclusion of the relative motion. In general, it could be concluded that at comparatively low speed there is little to choose between the six models, while as the speed goes up the differences increase. This is partly due to the differences in the abovewater hull shape. Another factor that must not be overlooked is that at the highest speed the wave added resistance constitutes only a very small part of the total resistance. Consequently, the stillwater resistance figures are more important to reckon with. Conversely, the wave added resistance at high speed is more difficult to extract from a model test and its measurement accuracy is lower than for the lower speeds. Nevertheless, Fig. 12 tells us that there exists a difference of some 20 percent between the various underwater hull forms, which would grow to 40 percent for the highest speed.

Effect of speed on pitching

A series of illustrations, Figs. 13–16, was included to show the effect of speed on pitching, which is the most dominant motion in head seas. One can see that as the speed goes up the pitch transfer function develops a rise around $\lambda/L = 2.0$, and for even higher speeds drops substantially in that wavelength range. The Doppler shift of the wave exciting moment relative to the pitch response function (viewed as a mass-spring oscillator) has much to do with this. The pitch transfer functions shown in the Figs. 13–16 have all been made nondimensional on the basis of wave slope, as is usual for an angular motion. An even more telling way to make it nondimensional is through dividing the pitch angle by ζ_a/L. If one does so, the transfer function assumes the illustrative peaked form that is better in line with observations, because it shows the occurrence of synchronous pitching better than on the basis of wave slope; see Fig. 18. This figure shows that for an increase in speed the pitch angle goes down dramatically, which is indeed what is observed in the experiment, and can directly be explained by the Doppler shift.

Effect of speed on other seakeeping quantities

The effect of speed on the other seakeeping quantities is shown in Figs. 17, 19, and 20 for Model 5 only. It is interesting to note that for heave at the lowest speed, the peak of the response function (heave as a mass-spring oscillator) very nearly coincides with the zero point of the wave exciting force. As the speed increases, heaving increases too for long waves, in particular in the range between the two lowest speeds. For this reason an extra speed was added between the two in subsequent experiments. The same great change between the lower two speeds is found in the acceleration, Fig. 19, where the peaks of the acceleration curves for the higher speeds are virtually on the same level. The wave added resistance in Fig. 20 exhibits a speed effect roughly proportional to the radical of the speed, and the Doppler shift as much in line with pitch as with the accelerations.

Some typical results on calm-water resistance

Some typical results of the resistance tests are shown in Fig. 37 for the Hull 5 (which was to become the parent hull). It shows the residuary resistance coefficient plotted on a basis of Froude number, the latter based on the third root of the displacement. One can see that the design speed of the series $F_n = 0.7$ to 1.0 ($F_{n\nabla} = 2.0$ to 3.0) coincides with the second hollow of the residuary resistance curve.

In the attending sinkage and trim diagram, Fig. 38, it is clearly visible that at first in the intermediate speed range the CG sinks in, associated with an increase in trim and likewise an increase in resistance, which works out to be the first hump around $F_{n\nabla} = 1.8$. In the design speed range the stern is lifted, resulting in a rise in CG and a trim angle around 1.5 deg. The resistance in this region benefits from this and exhibits a hollow, the second one.

Ship motion calculations

Calculations of the motions and resistance increase in waves are based on the well-known strip theory. In this way a two-

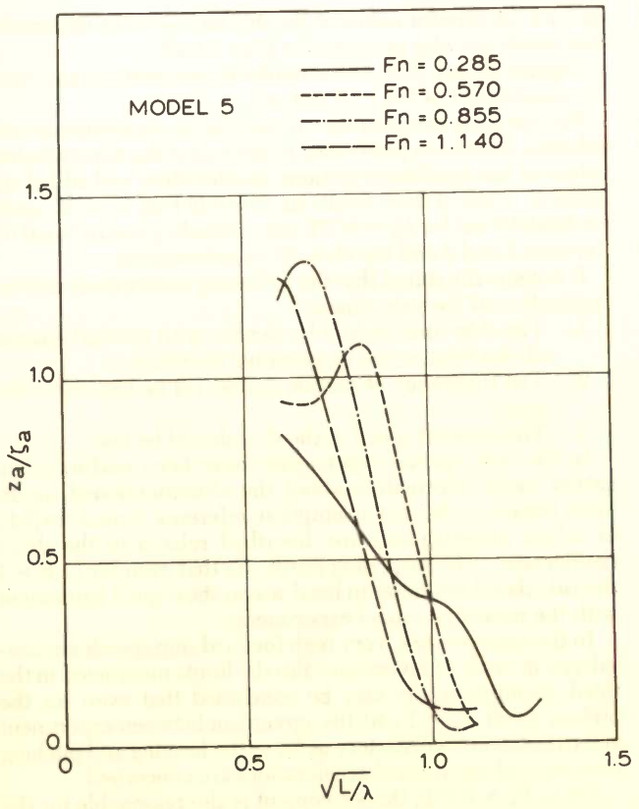

Fig. 17 Influence of speed on heave transfer functions for Model 5

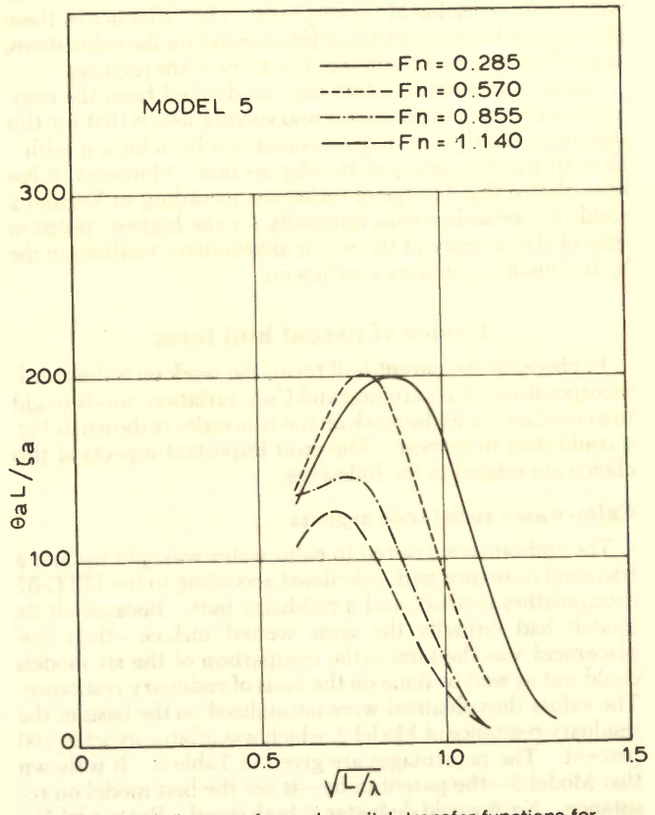

Fig. 18 Influence of speed on pitch transfer functions for Model 5

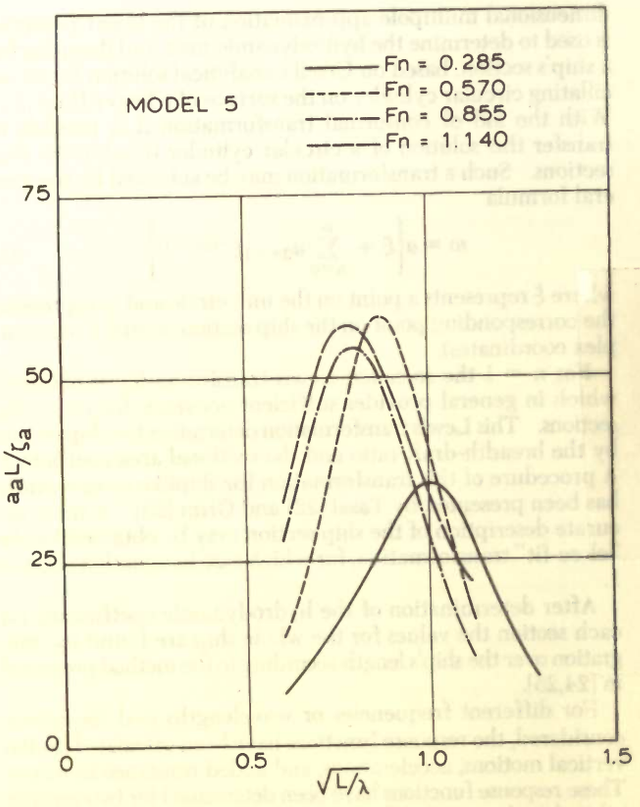

Fig. 19 Influence of speed on acceleration transfer functions for Model 5

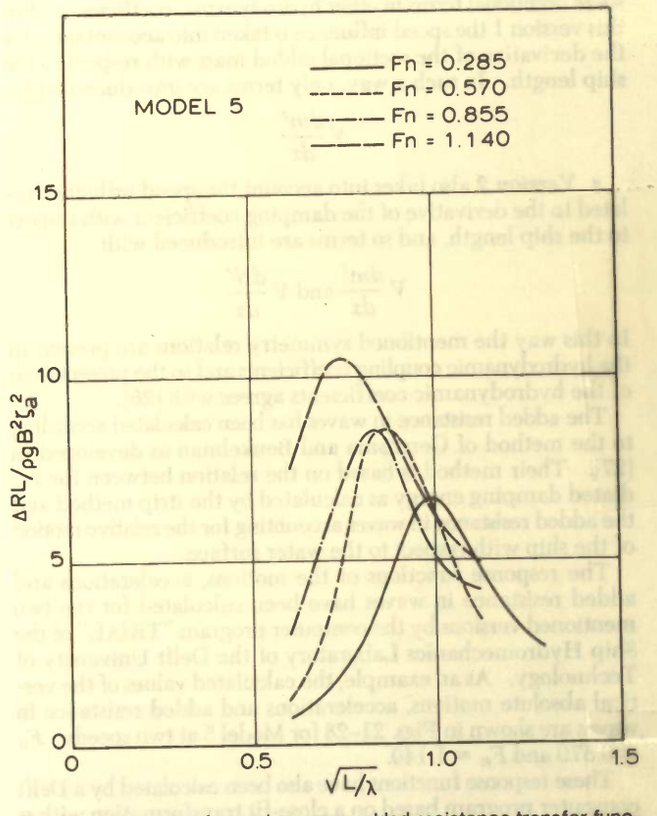

Fig. 20 Influence of speed on wave added resistance transfer functions for Model 5

dimensional multipole approximation of the linear potential is used to determine the hydrodynamic mass and damping for a ship's section, based on Ursell's analytical solution for an oscillating circular cylinder on the surface of a heavy fluid [21]. With the aid of conformal transformation it is possible to transfer this solution of a circular cylinder to arbitrary ship sections. Such a transformation may be achieved by the general formula

$$w = a\left\{\xi + \sum_{n=0}^{\infty} a_{2n+1}\xi^{-(2n+1)}\right\} \qquad (1)$$

where ξ represents a point on the unit circle and w represents the corresponding point on the ship section (w and ξ are complex coordinates).

For $n = 1$ the so-called Lewis transformation is obtained which in general provides sufficient accuracy for most ship sections. This Lewis transformation determines the ship section by the breadth-draft ratio and the sectional area coefficient. A procedure of this transformation for shiplike cross-sections has been presented by Tasai [22] and Grim [23]. A more accurate description of the ship section may be obtained by the "close-fit" transformation, for which case in equation (1), $n > 1$.

After determination of the hydrodynamic coefficients for each section the values for the whole ship are found by integration over the ship's length according to the method presented in [24,25].

For different frequencies or wavelengths and the speeds considered, the response functions have been calculated for the vertical motions, accelerations, and added resistance in waves. These response functions have been determined for two versions related to the speed influence as mentioned in [24] and [25]:

- *Version 1*, sometimes called the ordinary strip method (OSM), leads to a set of motion equations which lack some of the symmetry relations in the mass coupling coefficients and some additional terms in other hydrodynamic coefficients. For this version 1 the speed influence is taken into account only for the derivative of the sectional added mass with respect to the ship length. In such a way, only terms are introduced with

$$V\frac{dm'}{dx}$$

- *Version 2* also takes into account the speed influence related to the derivative of the damping coefficient with respect to the ship length, and so terms are introduced with

$$V\frac{dm'}{dx} \text{ and } V\frac{dN'}{dx}$$

In this way the mentioned symmetry relations are present in the hydrodynamic coupling coefficients and so the presentation of the hydrodynamic coefficients agrees with [26].

The added resistance in waves has been calculated according to the method of Gerritsma and Beukelman as developed in [27]. Their method is based on the relation between the radiated damping energy as calculated by the strip method and the added resistance in waves accounting for the relative motion of the ship with respect to the water surface.

The response functions of the motions, accelerations and added resistance in waves have been calculated for the two mentioned versions by the computer program "TRIAL" of the Ship Hydromechanics Laboratory of the Delft University of Technology. As an example, the calculated values of the vertical absolute motions, accelerations and added resistance in waves are shown in Figs. 21–28 for Model 5 at two speeds: $F_n = 0.570$ and $F_n = 1.140$.

These response functions have also been calculated by a Delft computer program based on a close-fit transformation with $n = 9$ in equation (1); this means that nine coefficients have been used for the transformation of the ship section to the unit circle. The results are also presented in Figs. 21–28.

Figures 29 and 30 show the results of computations and form the counterpart of Figs. 14 and 16.

For the same irregular seas as used for the experiments, calculations have been performed to determine the dimensionless values of the significant motions, accelerations and added resistance. Some of these results are shown in Figs. 33 to 36, again for Model 5 but for $F_n = 0.570$ only, including results based on Versions 1 and 2 and the close-fit transformation.

It is generally stated that the following assumptions restrict application of the strip theory:

1. The ship form should be slender with gradual change of this form in the longitudinal direction.
2. The frequency of motion should not be too low or too high.
3. The forward speed of the ship should be low.

In the past, special experiments have been performed to gather more information about the aforementioned limits. With respect to the first assumption, reference is made to [24], in which investigations are described related to the ship's slenderness. The surprising result was that even for $L/B = 4$ the calculated responses in head waves show good agreement with the measured model experiments.

In the present work, very high forward ship speeds are considered in order to investigate also the limits mentioned in the third assumption. It may be concluded that even for the highest speed, $F_n = 1.140$, the agreement between experiment and calculation is satisfactory as far as the heaving and pitching motions and the vertical accelerations are concerned.

Up to $F_n = 0.570$, this agreement is also reasonable for the relative motions and added resistance in waves. Above this speed, there is a considerable lack of agreement with respect to these phenomena. This might be due to the significant influence of the ship's own wave profile and dynamic swell-up, which is appreciable at these speeds. The influence of these phenomena has not been taken into account for the calculations, as yet further investigations in this respect are required.

Another conclusion which may be derived from the comparison between experiments and calculations is that for this ship form, hardly any improvement can be achieved with a close-fit transformation of the ship section. Moreover, it has been shown that the speed influence according to Version 2 yields less reliable results especially for the highest speeds in spite of the presence of the required symmetry relations in the hydrodynamic coupling coefficients.

Choice of parent hull form

In choosing the parent hull form, the work on Subseries 1, incorporating LCF variation and C_{WP} variation, was brought to a conclusion and the work on the true series as shown in Fig. 4 could start in earnest. The most important aspects of this choice are related in the following.

Calm-water resistance aspects

The resistance measured in calm water was split up into a frictional resistance part, calculated according to the ITTC-57 extrapolation method, and a residuary part. Because all six models had virtually the same wetted surface—their displacement was the same—the comparison of the six models could just as well be done on the basis of residuary resistance. The values thus obtained were normalized on the basis of the residuary resistance of Model 2, which was arbitrarily set at 100 percent. The percentages are given in Table 3. It is shown that Model 5—the parent to be—is not the best model on resistance. No. 6 would do better at high speed. But model No. 5 holds an attractive position:

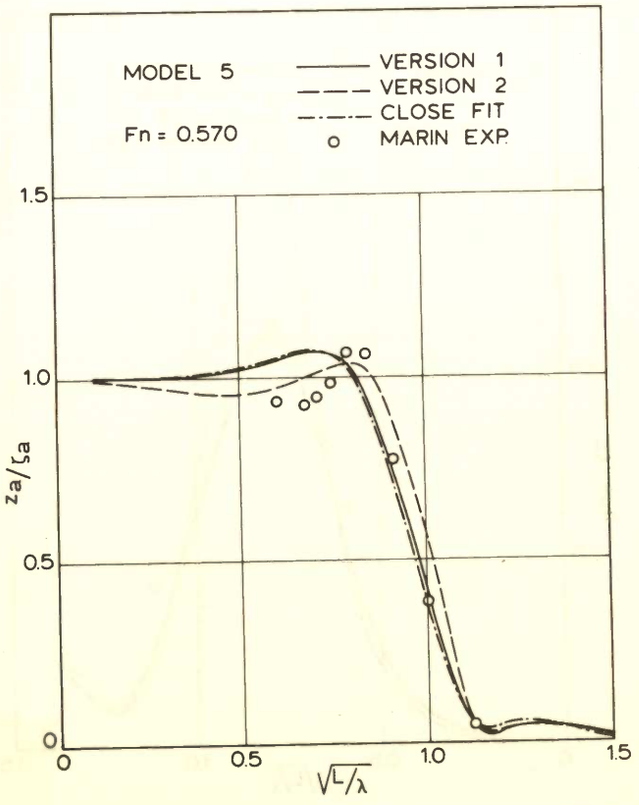

Fig. 21 Correlation of measurement to computation for heave transfer functions

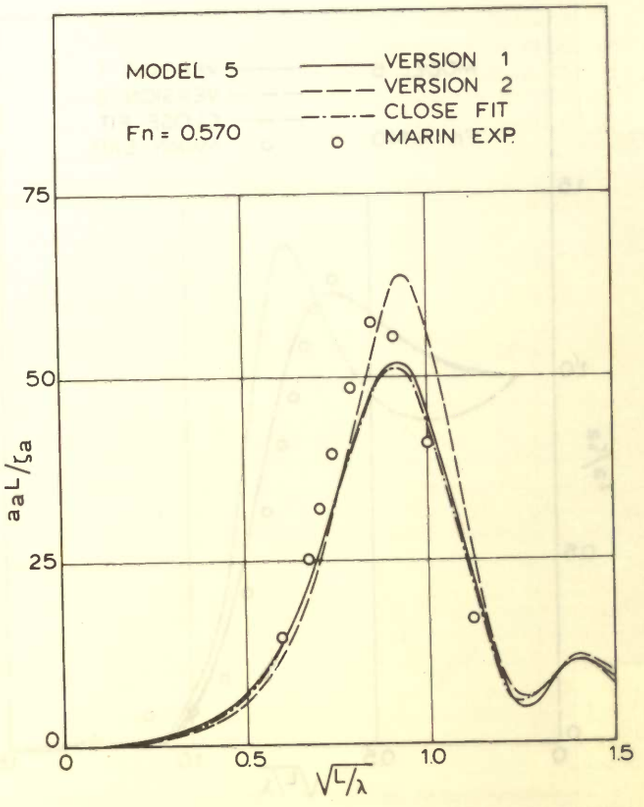

Fig. 23 Correlation of measurement to computation for acceleration transfer functions

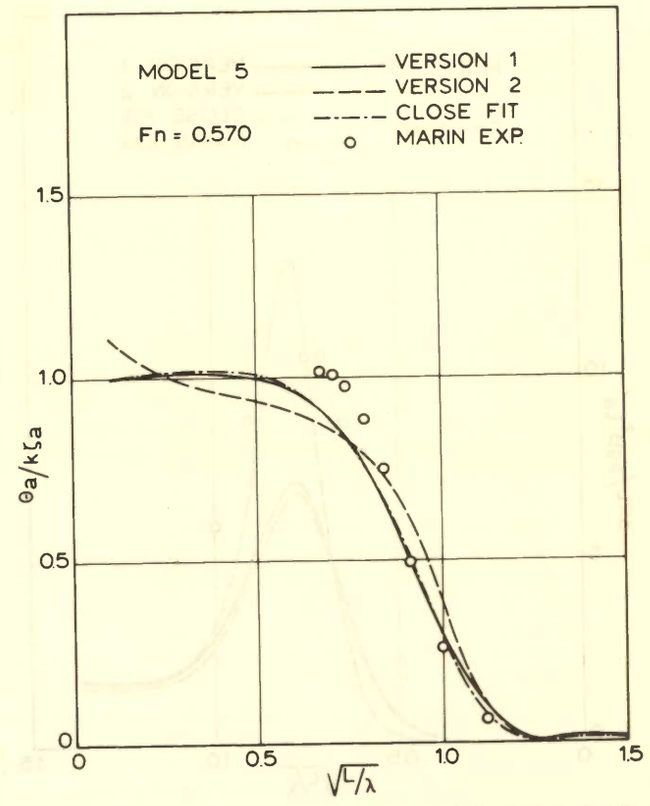

Fig. 22 Correlation of measurement to computation for pitch transfer functions

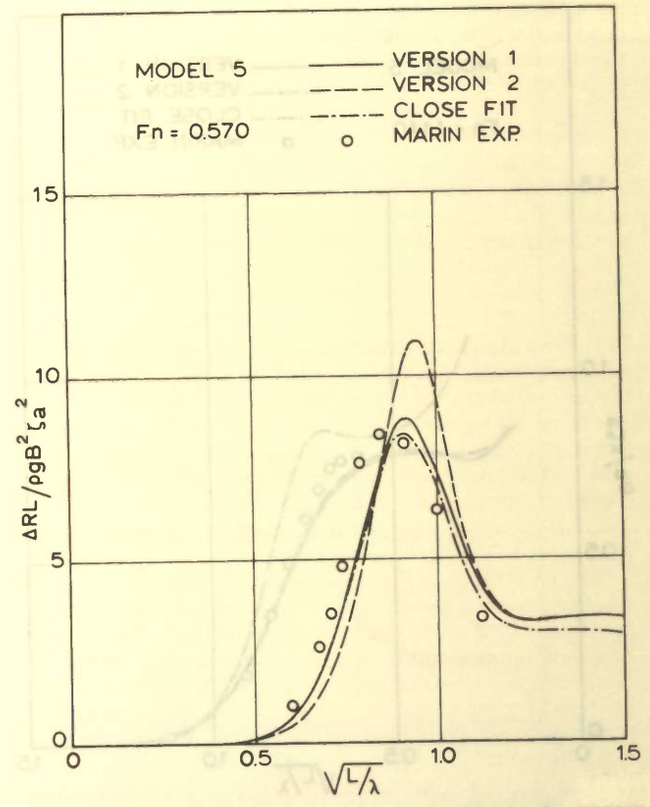

Fig. 24 Correlation of measurement to computation for wave added resistance transfer functions

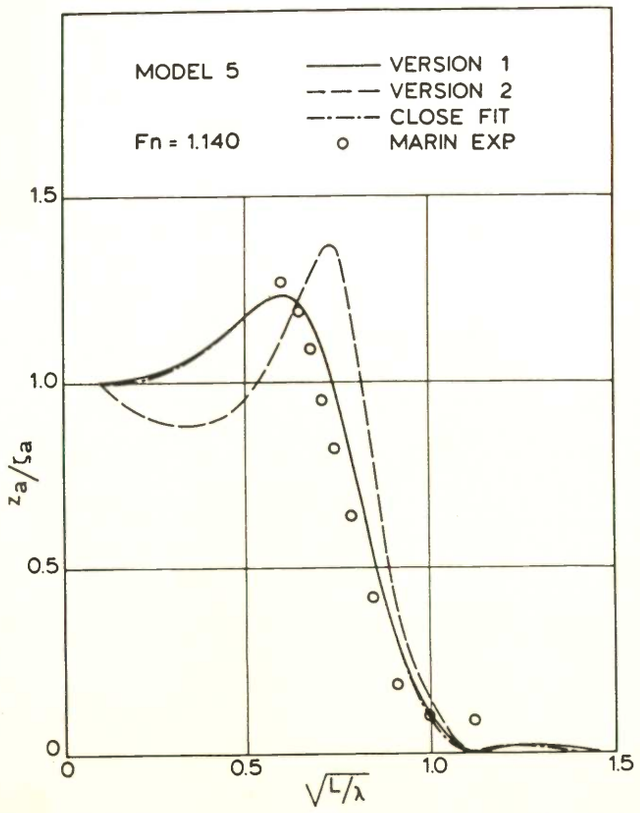

Fig. 25 Correlation of measurement to computation for heave transfer functions

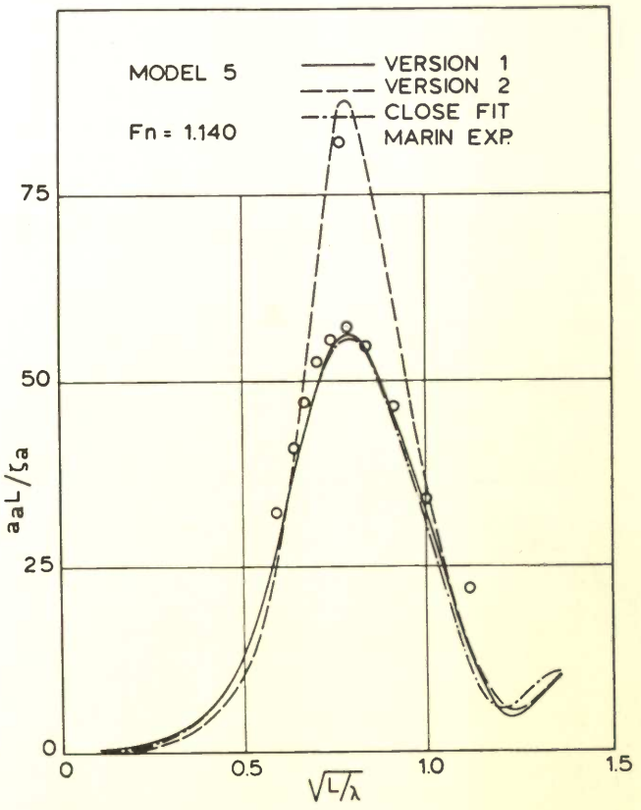

Fig. 27 Correlation of measurement to computation for acceleration transfer functions

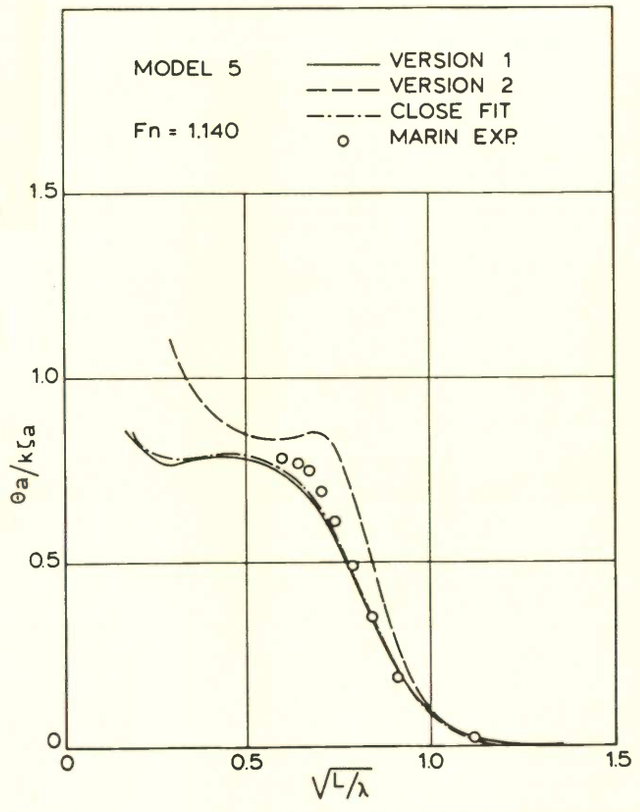

Fig. 26 Correlation of measurement to computation for pitch transfer functions

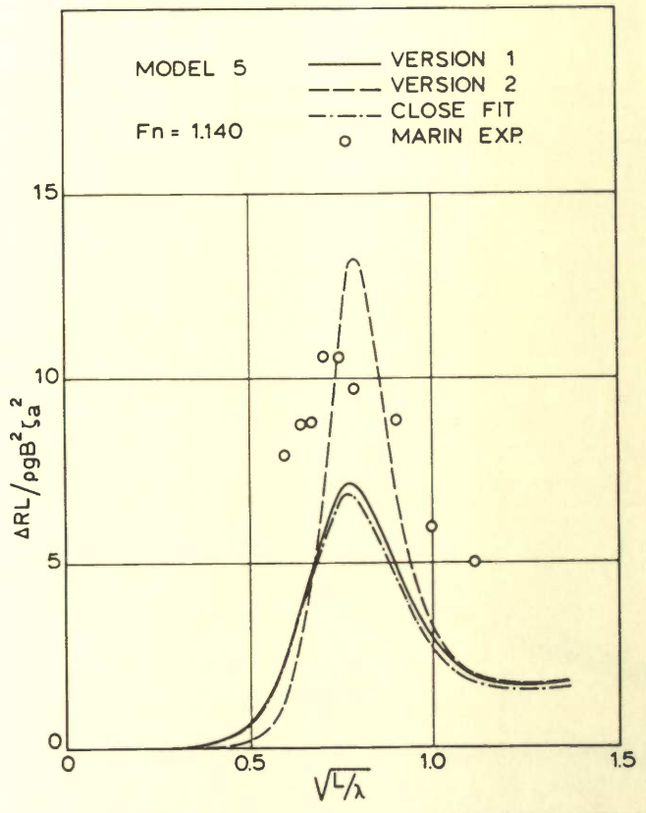

Fig. 28 Correlation of measurement to computation for wave added resistance transfer functions

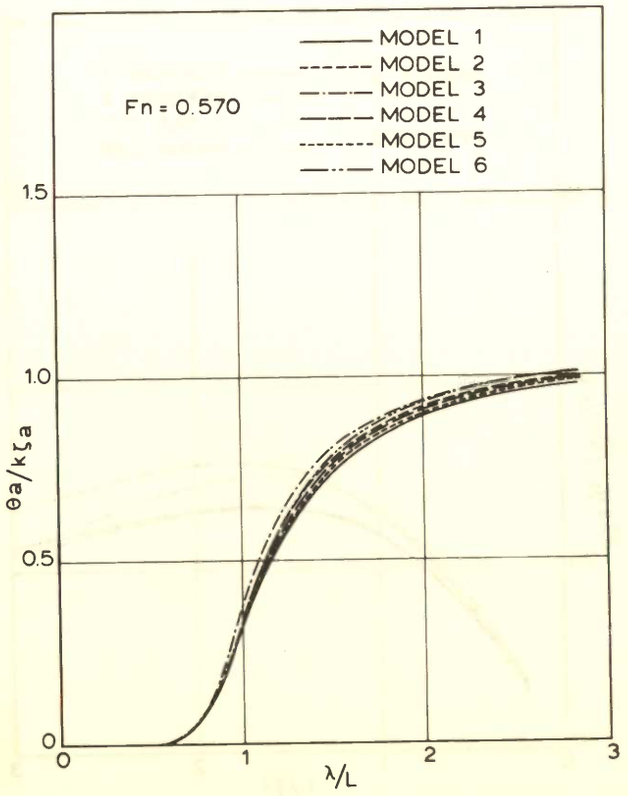

Fig. 29 Computed pitch transfer function comparison for six models

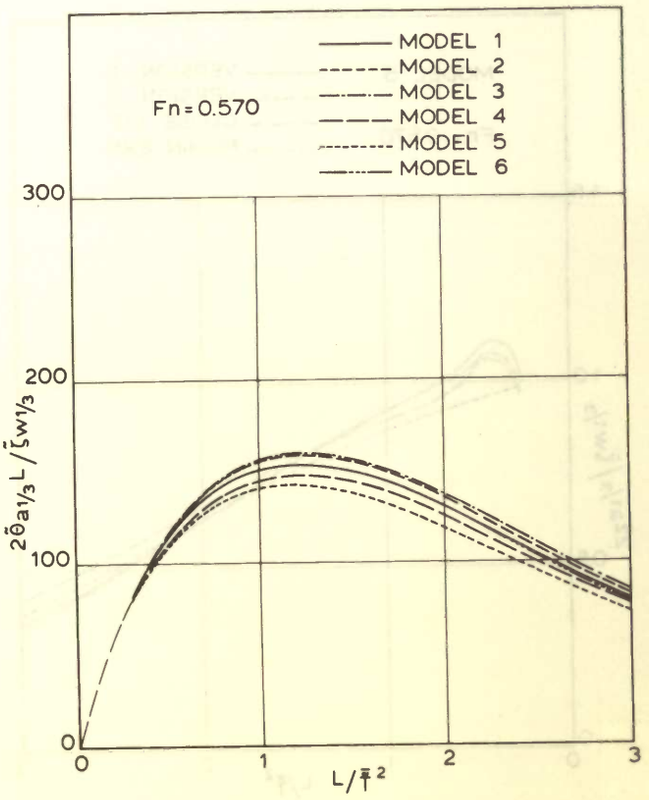

Fig. 31 Irregular transfer functions based on regular-wave tests

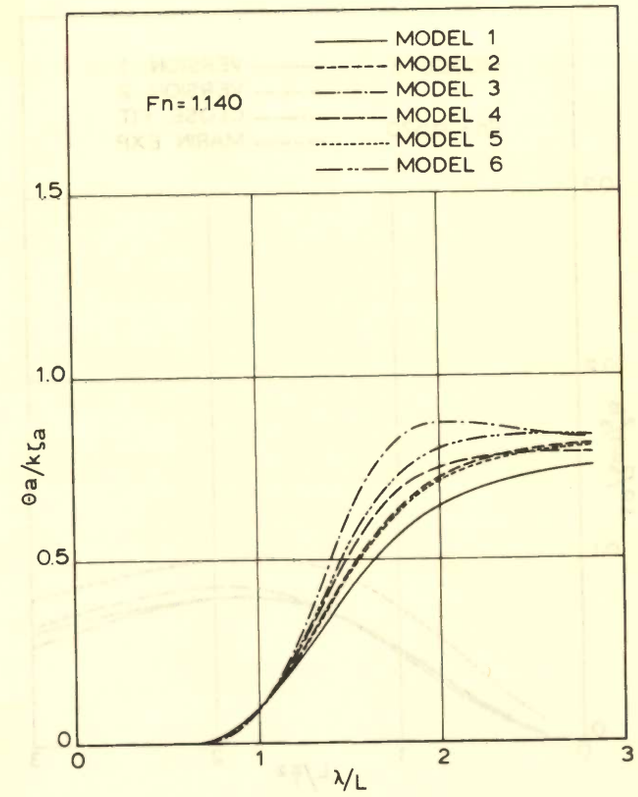

Fig. 30 Computed pitch transfer function comparison for six models

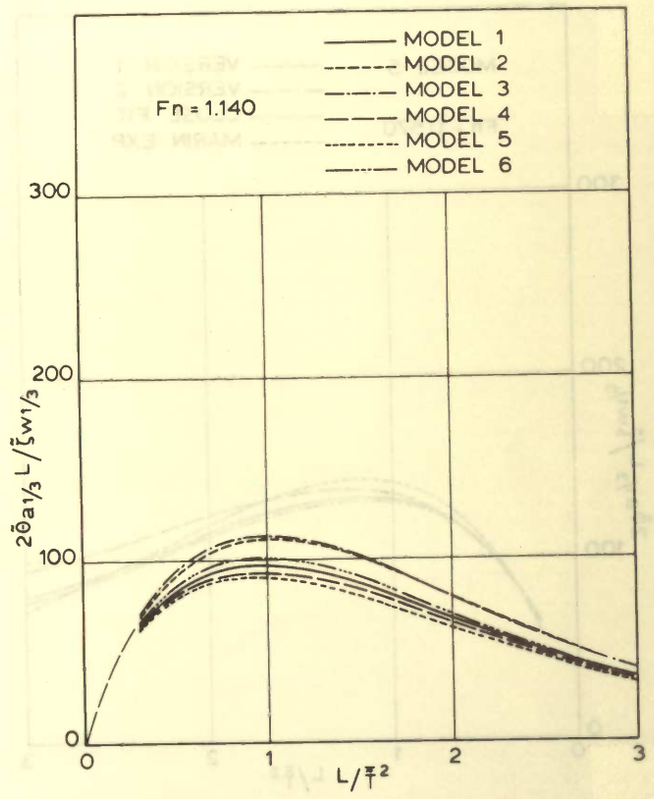

Fig. 32 Irregular transfer functions based on regular-wave tests

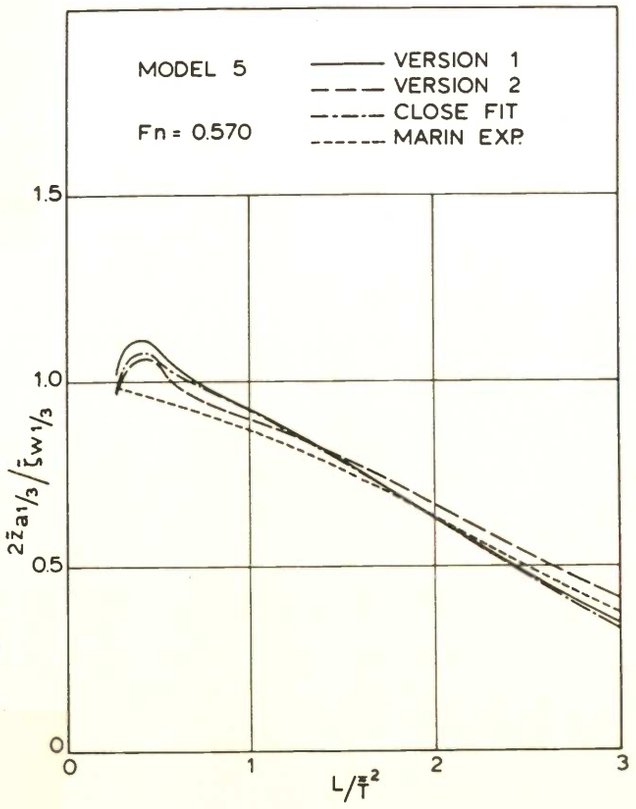

Fig. 33 Correlation of irregular transfer functions measured and computed for heave

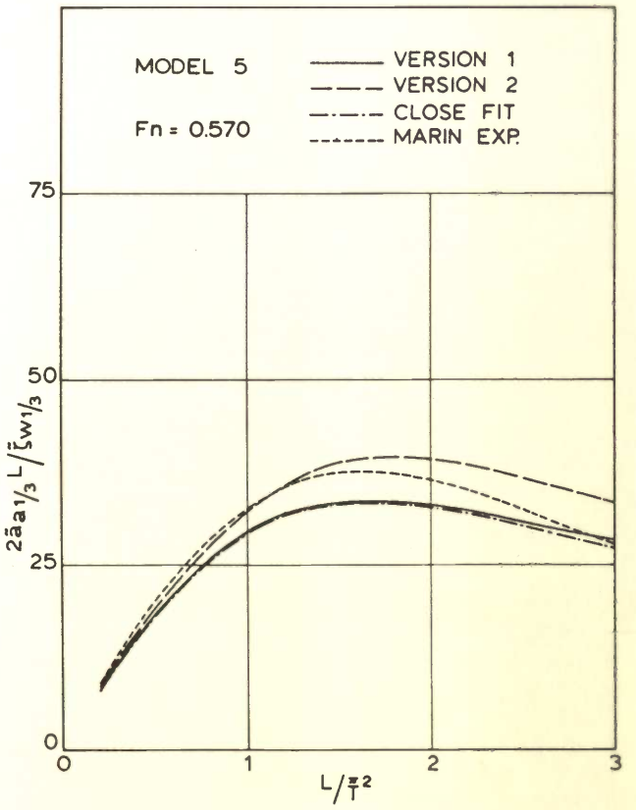

Fig. 35 Correlation of irregular transfer functions measured and computed for accelerations

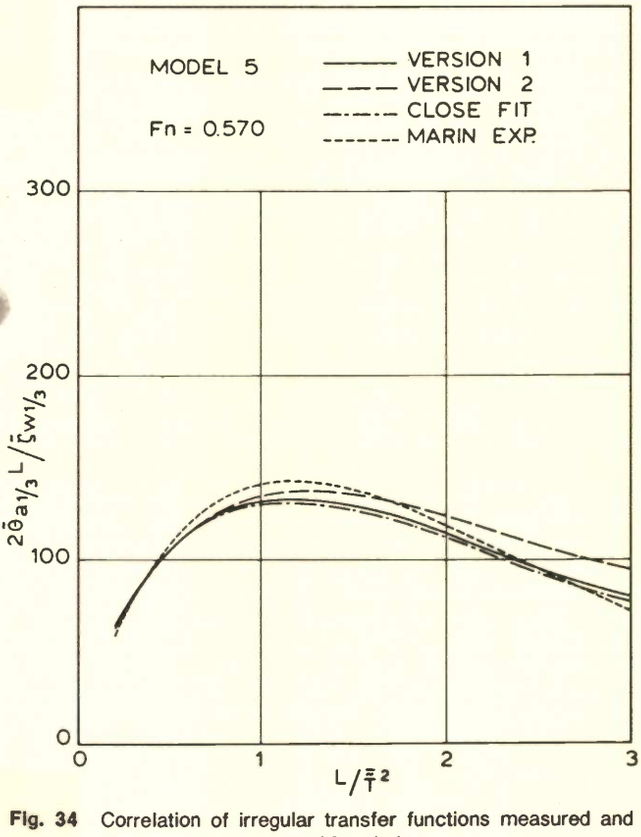

Fig. 34 Correlation of irregular transfer functions measured and computed for pitch

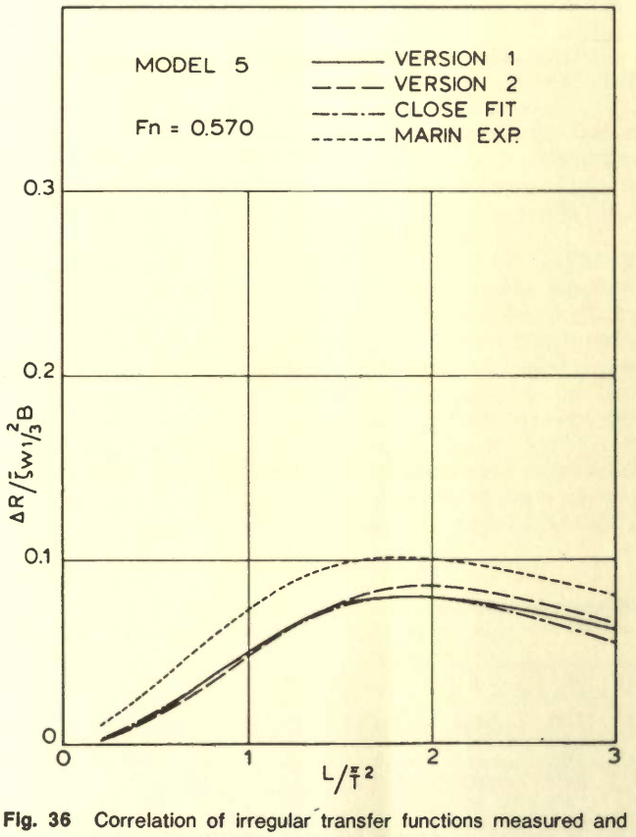

Fig. 36 Correlation of irregular transfer functions measured and computed for wave added resistance

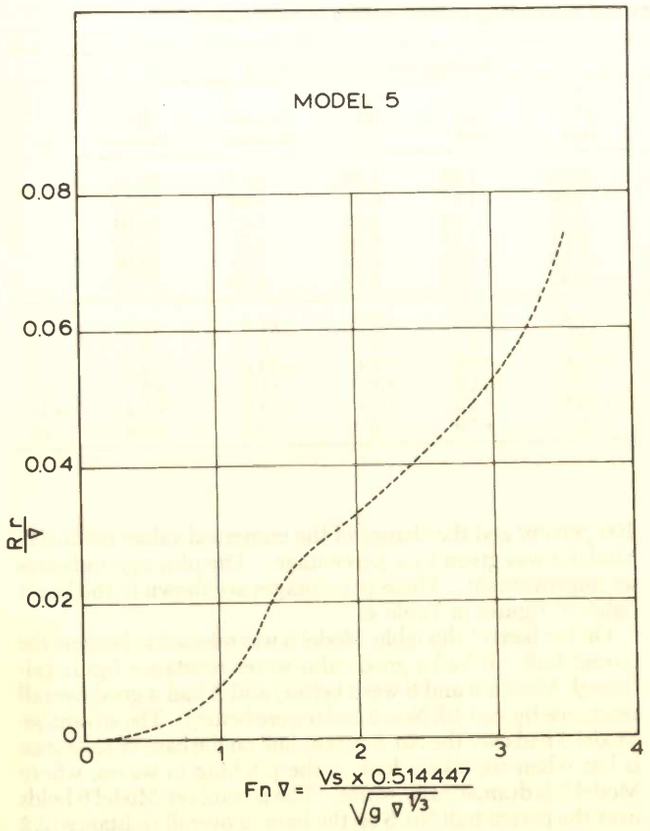

Fig. 37 Residuary resistance coefficient for Model 5

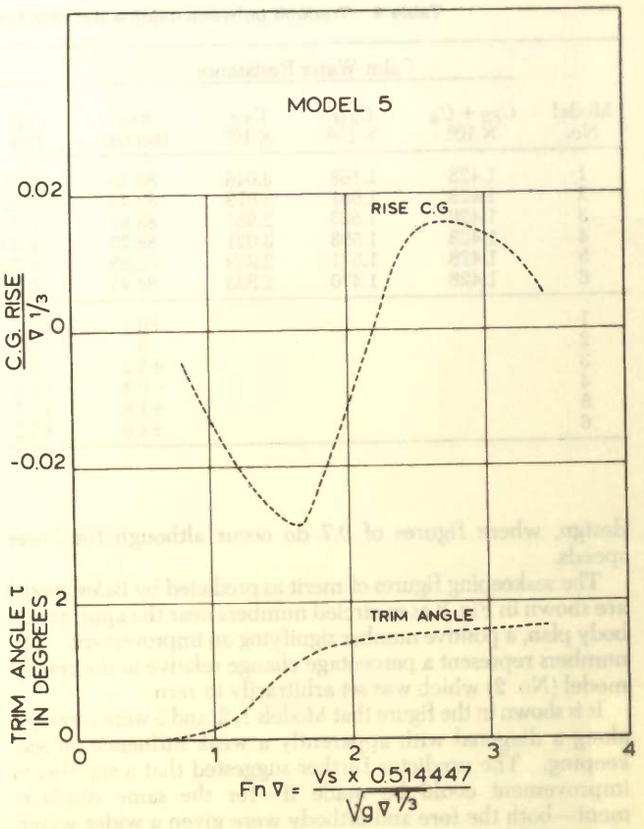

Fig. 38 Sinkage and trim in calm water for Model 5

- It is one of the three best on resistance at high speeds.
- It is very close to the best model at the design speed around $F_{n\nabla} = 2.5$.

So it is shown that a wide forebody combined with a medium-to-wide aftbody is good for residuary resistance.

Seakeeping aspects

In the foregoing a number of salient aspects in the field of seakeeping have been mentioned. For the selection of the parent hull it was necessary to obtain statistical data for irregular seas. To this end the measured transfer functions were synthesized with a family of wave spectra of unit significant wave height and a range of average periods. The result is a statistical measure, like the double significant output quantity presented in Figs. 31 and 32, representing a kind of transfer function for irregular seas. Although the diagrams embody the two-parameter ISSC wave spectrum and will be subject to change if a different spectral form is used, they nevertheless come in very handy for the comparison of ships, for design. As both parameters of the sea state, height and period, can be introduced independently of one another, it provides sufficient latitude to be used in practice.

For the choice of the parent hull, use was made of these kinds of diagrams as they are more straightforward than the transfer functions, which exhibit crossover points, making an assessment more cumbersome.

Seakeeping figure of merit

In the selection of the parent hull form, use has been made of Bales' regression model for destroyer-type ships [28]. For the purpose of comparing hull forms on their seakeeping merits, he had devised a regression predictor model based on a great number of hull shapes. In this model a great number of seakeeping parameters such as heave, pitch and acceleration are amalgamated to arrive at one single figure of merit indicative of the overall seakeeping performance of a hull.

The validation of this model is also shown in [28] and stems from back-designing a hull shape which has seakeeping characteristics superior to any ship in the data set. This was accomplished with the predictor model that uses only the ship's main particulars and associated quantities.

At first, the predictor model was tried on our Models 1, 2 and 3 which, as shown in Fig. 3, constitute the diagonal, incorporating a shift in LCF. Earlier the work of Bales and Cummins [29] had indicated a sizable improvement of heave and pitch if the forebody C_{WPF} were to be increased. The improvement found from the experiments was not as great as had been expected, perhaps because C_{WPF} had not been increased enough. In the series, C_{WPF} was not taken any higher than 0.6 as it was felt that this would result in an important calm-water resistance increase of more than 10 percent at Froude numbers in excess of 0.5. The restriction on C_{WPF} is not made in current frigate

Table 3 Residuary resistance comparison, normalized on Model 2

Speed, $F_{n\nabla}$	Model No. 1	2	3	4	5	6
1.0	95.2	100	100.0	120.8	96.2	120.6
1.5	97.6	100	91.0	96.0	91.6	88.4
2.0	100.3	100	93.8	99.2	89.4	91.1
2.5	101.2	100	93.2	99.5	94.9	90.9
3.0	104.1	100	89.9	100.0	98.0	88.7
3.5	103.5	100	89.8	101.1	98.0	90.4

Table 4 Tradeoff between calm-water resistance and seakeeping characteristics in head waves

Model No.	Calm-Water Resistance $C_{FS}+C_A$ $\times 10^3$	C_{RM} $\times 10^3$	C_{TS} $\times 10^3$	R_{TS} (tonne)	Seakeeping Characteristics z (m) rms	θ (°) rms	s_{17} (m) rms	a_{19} (g) rms	R_{AW} (tonne)	R_T (tonne)	Ⓜ
1	1.428	1.168	3.046	88.39	0.36	0.66	1.66	0.26	6.77	96.15	
2	1.428	1.651	3.079	88.44	0.39	0.66	1.77	0.27	6.84	95.28	
3	1.428	1.553	2.981	83.87	0.39	0.73	1.94	0.29	7.77	91.64	
4	1.428	1.593	3.021	88.75	0.39	0.61	1.56	0.26	6.77	95.52	
5	1.428	1.511	2.939	86.85	0.36	0.59	1.69	0.25	7.11	93.96	
6	1.428	1.470	2.898	84.44	0.37	0.63	1.63	0.27	7.50	91.94	
1				+0.1	+7.7	+7.6	+6.2	+3.7	+1.0	−1.0	0
2				0	0	0	0	0	0	0	0
3				+5.2	0	−10.6	−9.6	−7.4	−13.6	+4.0	−1
4				−0.4	+2.6	+7.6	+11.9	+3.7	+1.0	+0	+6
5				+1.8	+7.7	+10.6	+4.5	+7.4	−3.9	+1.4	+13
6				+4.5	+5.2	+4.5	+7.9	0	−9.6	+3.6	+6

design, where figures of 0.7 do occur although for lower speeds.

The seakeeping figures of merit as predicted by Bales' model are shown in Fig. 3 as encircled numbers near the appropriate body plan, a positive number signifying an improvement. The numbers represent a percentage change relative to the central model (No. 2) which was set arbitrarily to zero.

It is shown in the figure that Models 1, 2, and 3 were arranged along a diagonal with apparently a weak influence on seakeeping. The predictor further suggested that a significant improvement could be made if—for the same displacement—both the fore and aftbody were given a wider waterplane. This appeared a logical step because the draft and freeboard remain the same and so do the slamming and green water aspects. A wider waterplane overall suppresses heaving and pitching. The forebody C_{WPF} was still not allowed to go any higher than 0.6.

The suggestion cast by the figure-of-merit predictor was taken up and the three models in the right-hand top corner of Fig. 3 off the diagonal were also tested, denoted Models 4, 5 and 6. The results of the experiments appear to bear out the improvement projected by the prediction model, as the test results and the discussion on the seakeeping aspects have shown.

Tradeoff between calm-water resistance and seakeeping characteristics in head waves

Eventually the resistance properties of the six models had to be traded off against their respective behavior in head waves. This tradeoff, or the choice of the parent hull, was made in the following way.

A dimensional numerical design point was selected having the following particulars:

Length: 85 m (279 ft)

Speed: 48 knots

$F_n = 0.855$

$F_{n\nabla} = 2.49$

Sea state 4: $\xi_{w1/3} = 2.50$ m (8.20 ft)

$\bar{T}_1 = 7.00$ s

For this nominal point the calm-water resistance, the wave added resistance, and the total resistance were determined as well as the seakeeping determinants: heave, pitch, relative motion at station 17 and vertical acceleration at station 19.

The values are given in Table 4 for all six models, in the upper figures. In order to weigh the different quantities and to select the best model, the central model (No. 2) was arbitrarily set to 100 percent and the change of the numerical values relative to Model 2 was given by a percentage. The plus sign indicates an improvement. These percentages are shown in the lower batch of figures in Table 4.

On the basis of this table, Model 5 was selected to become the parent hull. It had a good calm-water resistance figure (although Models 3 and 6 were better) and it had a good overall resistance figure (still Nos. 3 and 6 were better). The advantage Model 3 had over the No. 5 parent hull on the basis of resistance is lost when we take a look at the pitching in waves, where Model 3 is dramatically worse. The advantage Model 6 holds over the parent hull No. 5 on the basis of overall resistance (2.2 percent) is, in our view, outweighed by the significantly better seakeeping characteristics of heave, pitch and accelerations of Model 5. The relative motion figure of No. 5 is somewhat in want, but could easily be rectified by a small change to the abovewater flare forward.

So, taking everything together, Model 5 is selected because it is 6 to 20 percent better on pitching as compared to the next models in line (Nos. 3 and 6) at the expense of a 2 percent penalty on overall resistance in waves.

In the last column of Table 4 the seakeeping figure of merit Ⓜ that Bales [28] computed for these models is given. This figure not only led to the extension of this subseries to include Models 4, 5 and 6, but it also pointed out the most prospective parent hull. In addition to this, other nominal design points were tried for a smaller and a bigger ship, in a different sea state, but again hull form No. 5 came out as the best balance between calm-water resistance and seakeeping aspects.

Continuation of the systematic series work

State of affairs

The experiments related in the paper cover a forerunner series of six models that led to the selection of a parent hull. With that the parameters-to-be-fixed were established and work on the true series as mentioned earlier and elucidated by its parameter space in Fig. 4 could begin in earnest. This work is in an advanced stage, with 15 of the 27 models having been tested. While all this is in progress, a continuation is in the offing in the sense of a subseries devoted to a variation of prismatic coefficients and a series on trim wedges, on longitudinal radius of gyration, possibly on spray-rails, and more than likely on propulsion, struts, shaft position and related topics.

Transformation program

The systematic series of hull forms as shown in Fig. 4 re-

quired a transformation procedure to obtain the lines of all the models as logical derivatives of the parent hull form. The first step was to computerize the parent hull form itself with its local details. The second step was the transformation routine itself. For L/B and B/T transformations the problem was quite easily solved by stretching and widening the hull shape. For the block coefficient variation it was first necessary to determine how to go about it, either through a change in C_P or C_M.

An additional problem to be solved was the transformation of the abovewater hull form. As the underwater hull form changes in a consistent fashion, the angle of intercept between the sections and the waterplane changes. It was found that shaping the abovewater hull in a systematic fashion had to be done quite independently from the underwater hull form in order to avoid hulls with a very wide forebody overhang or with hardly any flare at all.

Eventually a transformation program resulted that can—within the boundaries set by the series parameters and its characteristic hull shape—vary L/B, B/T, C_B, C_p, C_M, C_{WP} and C_{VP}, so as to interpolate to any set of parameters within the cube matrix.

Numerical data base

The calm-water resistance data as well as the seakeeping data obtained will be put into design charts in as condensed a form as possible.

To make the maximum use of the data in obtaining an optimum hull for a given set of design requirements, the data set will also be computerized, so that with the use of a search and interpolation routine the required hull can be obtained along with its resistance and seakeeping characteristics with a minimum of effort.

Concluding remarks

For the twofold purpose of obtaining design data on high-speed hull forms in the areas of both calm-water resistance and seakeeping and to investigate what the prospects are for displacement hulls in the extremely high-speed range, a systematic series of hull forms has been discussed. It was found that a hull can be obtained that incorporates a sizable improvement in seakeeping at the expense of just a little extra resistance.

In the light of the currently growing belief, expressed in many a contemporary paper, that seakeeping does matter and does have an impact on ship operation, this information may be of further assistance in assessing the inevitable tradeoff to be made when more emphasis is to be laid upon seakeeping behavior.

Acknowledgment

The work reported herein, covering the initial steps toward the full series of hull forms, has been funded by the Royal Netherlands Navy and by the Maritime Research Institute Netherlands (NSMB Wageningen/Ede Laboratories). The considerable assistance of the Royal Netherlands Navy and of the David W. Taylor Naval Ship Research and Development Center (DTNSRDC), acting on behalf of the Office of Naval Research, at this stage, and their both becoming a sponsor of the series proper, is gratefully acknowledged.

In particular, the assistance rendered by the late Nathan K. Bales of DTNSRDC during the initial stages of the project and the deliberations leading up to the choice of the parent hull is most gratefully recalled.

References

1 Tritton, D. J., *Physical Fluid Dynamics*, Van Nostrand Reinhold (U.K.), 1982.

2 Merk, H. J., "Fysische Stromingsleer," Lecture Notes, Delft University of Technology, The Netherlands, 1982.

3 Comstock, E. N. and Keane, R. G., Jr., "Seakeeping by Design," *Naval Engineers Journal*, April 1980.

4 Comstock, E. N., Bales, S. L., and Keane, R. G., Jr., "Seakeeping in Ship Operations," SNAME Spring Meeting/STAR Symposium, 1980.

5 Kehoe, J. W., "Destroyer Seakeeping: Ours and Theirs," *Proceedings*, United States Naval Institute, Nov. 1973.

6 Kehoe, J. W., Brower, K. S., and Comstock, E. N., "Seakeeping," *Proceedings*, United States Naval Institute, Sept. 1983.

7 Olson, S. R., "An Evaluation of the Seakeeping Qualities of Naval Combatants," *Naval Engineers Journal*, Feb. 1978.

8 Mandel, P., "Seaway Performance Assessment for Marine Vehicles," Sixth AIAA Conference on Marine Systems, American Institute of Aeronautics and Astronautics, Sept. 1981.

9 "Helicopter Operations from Small Ships," *Combat Craft*, July 1983.

10 "Certification of Helicopters for Use on Board Ship," Netherlands Aerospace Laboratory, Europort Conference on Naval Construction and Equipment, Amsterdam, 1978.

11 Eames, M. C., "Advances in Naval Architecture for Future Surface Warships," *Trans.* RINA, 1980.

12 Mantle, P. J., "Cushions and Foils," SNAME Spring Meeting, Philadelphia, 1976.

13 "Status of Hydrodynamic Technology as Related to Model Tests of High-speed Marine Vehicles," High Speed Marine Vehicle Panel, 16th International Towing Tank Conference, 1981.

14 Rader, H. P., "Wasserfahrzeuge für hohe Geschwindigkeiten," *Schiff und Hafen*, Heft 3, 1981.

15 Comstock, E. N., Bales, S. L., and Gentile, D. M., "Seakeeping Performance Comparison of Air Capable Ships," *Naval Engineers Journal*, April 1982.

16 Silverleaf, A. and Cook, F. G. R., "A Comparison of Some Features of High Speed Marine Craft," *Trans.* RINA, 1970.

17 Bailey, D., "The NPL High Speed Round Bilge Displacement Hull Series," *Trans.* RINA, 1976.

18 Yeh, H. Y. H., "Series 64 Resistance Experiments on High-speed Displacement Forms," *Marine Technology*, Vol. 2, No. 3, July 1965.

19 Lindgren, H. and Williams, A., "Systematic Tests with Small, Fast Displacement Vessels, including a Study on the Influence of Spray Strips," SNAME Diamond Jubilee International Meeting, 1968.

20 Johnson, "The Changing Design Process," *Naval Engineers Journal*, April 1980.

21 Ursell, F., "On the Virtual Mass and Damping of Floating Bodies at Zero Speed Ahead," *Proceedings*, Symposium on the Behaviour of Ships in a Seaway, Wageningen, The Netherlands, 1957.

22 Tasai, F., "On the Damping Force and Added Mass of Ships Heaving and Pitching," *Reports of Research Institute for Applied Mechanics*, Kyushu University, Japan, 1960.

23 Grim, O., "A Method for a More Precise Computation of Heaving and Pitching Motions, Both in Smooth Water and in Waves," *Proceedings*, Third Symposium on Naval Hydrodynamics, Scheveningen, The Netherlands, 1960.

24 Gerritsma, J., Beukelman, W., and Glansdorp, C. C., "The Effect of Beam on the Hydrodynamic Characteristics of Ship Hulls," *Proceedings*, Tenth Symposium on Naval Hydrodynamics, 1974.

25 Beukelman, W., Huijsmans, R. H. M., and Keuning, P. J., "Calculation Methods of Hydrodynamic Coefficients of Ships in Shallow Water," Ship Hydromechanics Laboratory, Delft Hydraulics Laboratory, Maritime Research Institute, Report No. 571-A, 1983.

26 Salvesen, N., Tuck, E. O., and Faltinsen, O. M., "Ship Motions and Sea Loads," TRANS. SNAME, Vol. 79, 1970.

27 Gerritsma, J. and Beukelman, W., "Analysis of the Resistance Increase in Waves of a Fast Cargo Ship," *International Shipbuilding Progress*, 1972.

28 Bales, N. K., "Optimizing the Seakeeping Performance of Destroyer-type Hulls," *Proceedings*, 13th Symposium on Naval Hydrodynamics, Japan, 1980.

29 Bales, N. K. and Cummins, W. E., "The Influence of Hull Form on Seakeeping," TRANS. SNAME, Vol. 78, 1970.